PART – A

Geochemical study of sediments from the Western Continental Margin of India

Chapter 1

Introduction

The role of continental margins in regulating the marine geochemical cycles of elements and as a repository of high resolution records of climate and environmental history is getting increasingly recognized. The primary components of margin sediments are weathering products delivered by rivers and biogenic materials settling from the overlying water-column. Some of the recent studies (Martin and Windom, 1991; Milliman,1991) indicate that bulk of the suspended sediments delivered by the rivers to the ocean are deposited in the ocean margins and only less than one fourth of this supply escapes to the open ocean. The biological productivity along the margins is generally high due to higher rates of nutrient input via rivers and coastal upwelling processes. This biological productivity contributes significantly to the organic matter, $CaCO_3$ and opal content of the sediments. Thus, margins sites, in general, have high rates of sediment accumulation (typically a few mm/y) of terrigenous and biogenic materials. These sedimentation rates are orders of magnitude higher than those observed in typical open ocean areas (Goldberg and Koide,1962; Rosholt et al,1961). Therefore, it is possible to retrieve high resolution records of climatic and environmental conditions during the past few centuries from the study of margin sediments.

The sediments in margin areas are usually rich in organic matter resulting from the high biological productivity in the overlying water column. Recent estimates of the primary production suggests that about 18–30 % of world ocean productivity occurs in the shelf regions (Wollast,1991; Martin and Thomas,1994). These values are very significant since the margins occupy only 7% of the total ocean surface. It has been inferred that about 80% of primary production in margin regions is sustained by recycling of nutrients (Martin and Thomas,1994); the remaining being "new production" resulting from supply of nutrients either from riverine, atmospheric or upwelled deep waters. Spitzy and Ittekkot (1991) have estimated that the global organic carbon input by rivers is lower by a factor of two compared to this new production. Likewise, based on the global nitrogen budget, it has been suggested that upwelling of deep waters is the major source of nutrients for the new production in the margin areas (Wollast,1993; Walsh,1991). Furthermore, the global geochemical mass-balance study of dissolved Cu, Cd, Ni and Zn in margin areas indicates that their inputs from upwelled waters exceed the combined inputs of the riverine and atmospheric sources (Martin and Thomas, 1994). These results, therefore, suggest that there is continuous exchange of the biogenic materials and trace metals between continental margins and the open ocean. These exchange processes and the associated magnitude and direction of fluxes of biogenic elements have been a subject of current interest in the Global Change Studies.

A significant fraction of organic matter depositing in the margin sediments undergoes diagenesis making the margins an active site of benthic sedimentary processes which affect the marine biogeochemical cycle of elements. Biodegradation of organic matter also results in sub-oxic/anoxic conditions in the overhead water-column as well as near the sediment-water interface. Such conditions influence to a great extent the mobility of redox sensitive elements, notably manganese and uranium within a sediment column. Similarly some of the particle reactive elements such as Pa, Po and Pb are sequestered in the margin sediments due to enhanced boundary scavenging processes (Bacon et al,1976; Anderson et al,1983). Thus, the study of margin sediments is useful in understanding the weathering history of adjacent land-mass, biological productivity in the water-column, recent anthropogenic inputs of materials, and exchange of various elements between the coastal margins and the open ocean.

In this context, sediments from the Western Continental Margin of India (WCMI) are important as they underlie a unique marine geochemical province of the eastern Arabian sea. The two Indian monsoons, southwest (SW) and northeast (NE), result in reversal of surface ocean currents both in magnitude and direction. The SW monsoon being far more intense causes extensive upwelling in many regions of the Arabian sea. The upwelling induces high biological productivity in water-column which, in turn, causes significant rain of organic matter to the sediments. The combustion of organic matter during its transit through the water-column and also in sediments dictates the profiles of dissolved oxygen, nitrate, nitrite, sulphate and other chemical constituents both in seawater and in sediment pore water. A unique feature of the Arabian sea is the presence of a sub-oxic layer in the intermediate depths associated with intense denitrification (Naqvi,1994). It is expected that the distribution of particle-reactive and redox sensitive elements in the water column and sediments would be significantly influenced by these conditions. In addition, three west flowing rivers of the Indian sub-continent, the Indus, Narbada and the Tapti supply large amount of sediments and nutrients to the Arabian sea. The annual discharge of suspended load by the Indus river to the Arabian sea is about 1×10^8 tons (Milliman and Meade,1983) whereas the Narbada and Tapti together account for 0.6×10^8 tons (Borole et al,1982a). The fluvial material derived from these rivers is by and large deposited along the continental margin of the eastern part of the Arabian sea due to clockwise surface circulation during peak discharge periods (Ramswamy et al,1991). In addition to the river discharge, there is also significant input of aeolian dust into the Arabian sea (Goldberg and Griffin,1970; Kolla et al,1981; Sirocko and Sarnthein,1989).

A number of studies on the surface-sediments from the Western Continental Margin of India have been reported. These studies focus primarily on the chemical and mineralogical composition of the sediments (Nair,1969; Rao,1978; Nair and Hashimi,1980,1981; Nair et al,1982; Borole et al,1982a; Gupta and Hashimi,1985; Paropkari et al,1992); particularly the spatial variations in the abundances of $CaCO_3$, Mg, Mn, organic carbon, clay-minerals and some trace elements. Broadly, these variations have been ascribed to weathering of adjacent land-mass, mixing of relict calcareous materials with those depositing from the water-column, spatial variations in the water-column productivity and influence of external forcings such as the tides and monsoonal winds. Rao (1978) has reported variations in $CaCO_3$ content of the inner shelf (water depth < 50 m) and the outer shelf sediments (water depth 50–100 m) where it ranges from 5–25% and 50–94%, respectively. Such variations have been interpreted in terms of relative contributions from recent terrigenous and relict calcareous materials in the outer shelf region (Nair and Hashimi,1980). In the same region, Nair and Hashimi (1981) have observed that aragonite is the dominant mineral followed by low and high magnesium calcites in sediments and oolitic limestone samples. Earlier studies have reported enrichment of U (Borole et al,1982b) in anoxic shelf and slope sediments indicating its authigenic removal from seawater whereas Mn diffuses out under reducing conditions (Borole et al,1982a). Such studies point out the importance of these margin sediments as both source and sink for trace elements. Although, the distribution of organic carbon in sediments of the Arabian sea shows a broad correlation with surface productivity, the two do not appear to be directly coupled (Paropkari et al, 1992). High organic carbon ($> 4\%$) is generally found in the upper slope sediments whereas moderate carbon content ($1-4\%$) is observed in the lower slope regions. Lower organic carbon ($< 1\%$) is reported in deep Arabian sea sediments beyond the lower slope. Critical evaluation of the spatial variability in the organic carbon content reveals that its high abundance coincides with the oxygen minimum zone in the overlying water-column suggesting its better preservation (Paropkari et al, 1992).

Although the riverine contribution of sediments to the eastern Arabian sea, spatial variability in mineralogic composition and elemental abundances of surface sediments are well documented and understood, there are major gaps in the understanding and interpretation of the temporal variability of redox sensitive elements (e.g. U, Mn, Fe). Also, the spatial variability of some of the particle reactive nuclides (e.g. ^{232}Th, ^{230}Th, ^{210}Pb) in the margin regions of western India and the processes controlling their distribution need to be understood.

Goals of the present study

In this study, an attempt has been made to determine the depositional fluxes of selected sedimentary constituents during the past few centuries and their relation to chemical properties, and biogeochemical processes occurring along the WCMI. This has been accomplished through geochronological and geochemical studies of sediment cores collected from this region. The specific objectives are:

(i) to determine the spatial and temporal variations in the abundances and depositional fluxes of selected sedimentary components and elements along the WCMI;

(ii) to assess the role of these sediments in sequestering and/or supplying elements to the Arabian sea interior;

(iii) to infer environmental changes, if any, that have occurred along the margin during the past few centuries.

With these objectives sediment cores were collected from the WCMI and analyzed for a suite of elements and natural radioactive isotopes belonging to U–Th series. This study is presented in the following chapters: Chapter 2 describes the experimental details and analytical procedures that were adopted. Chapter 3 deals with results and discussion followed by a summary in Chapter 4.

Chapter 2

Experimental Techniques

In order to evaluate the role of sediments from the WCMI in sequestering and/or releasing natural radionuclides and selected transition metals to the eastern Arabian sea, several short cores were collected and analyzed for various chemical constituents. The Arabian sea is strongly influenced by atmospheric forcing driven by the SW and NE Indian monsoon winds which cause seasonal oscillations in upwelling and primary productivity regimes. Recent study of Shetye et al (1990) has shown that the coastal circulation pattern during SW and NE monsoons is driven by local forcings such as the wind stress and hydrodynamic pressure gradients. The circulation pattern in the eastern Arabian sea as inferred from the hydrographic data (temp., salinity, and density) collected during the SW monsoon (1987) is similar to that of eastern boundary currents in which surface current flows along the longshore component of the wind stress (Shetye et al,1990). However, during the NE monsoon the coastal current flows against the longshore component of the wind stress (Shetye et al,1991).

A typical characteristic of the eastern boundary current is that surface ocean waters experience high photosynthetic activities and deep waters are anoxic or sub-oxic. The supply of nutrients e.g. PO_4–P and NO_3–N to upper layer of ocean is largely controlled by upwelling besides regenerative supply by local bacterial activity. The average annual column productivity (100 m water depth) between 20–25°N and 60–70°E ranges from 0.5 to 1 $gC/m^2 \cdot d$ (Quasim,1977). The intermediate waters of the Arabian sea are characterized by sub-oxic/denitrification layer. Paradoxically, the most intense denitrification is reported to occur not beneath the areas of high productivity but below regions of relatively weaker productivity along the continental margin (Naqvi,1994). Such features are distinctly different from other oceanic regions such as the eastern tropical Pacific ocean which is characterized by biologically productive surface waters and denitrifying zone in deeper layers.

2.1 Sampling

The above mentioned features of the eastern Arabian sea make it pertinent to study the spatial and temporal variations in the biogenic and trace elemental composition of the margin sediments. In this context, five sediment cores viz. L-8, J-7, I-5, K-11 and M-12 (Fig. 2.1), each of ~25 cm length, were raised in Dec 1988 during the 47th cruise of ORV Sagar Kanya. All these cores were collected using a spade corer (size 50×30× 20 cm) to minimize mixing of surface sections during coring. Another core 2502 (Fig. 2.1) of ~1 m length was collected using a gravity corer during Feb 1992. This core was studied upto a length of ~30 cm from the surface. The four cores, (L-8, J-7, I-5 and 2502) are from the upper slope region with water depth ranging from 280 to 350 m, where the core of denitrification layer (centered at ~300 m depth, Naqvi et al., 1990) meets the sediment-water interface. The remaining two cores, viz. K-11 and M-12 are from the lower slope where water depth is ~2500 m (Table 2.1). Immediately after collection, sub-cores of ~5 cm diameter and ~25 cm in length were sampled and subsequently the cores were cut into 1−2 cm sections for the top 10 cm length and remaining part into 2 cm sections.

The physical texture of the cores indicates that they are composed of calcareous mud. In few cores, the presence of anoxic conditions just below the sediment-water interface was evident from the smell of H_2S during sampling (Table 2.1). Such sediments, because of their anoxic nature are unlikely to be influenced by bioturbation and hence are better suited for obtaining chronological information of the margin geochemical processes.

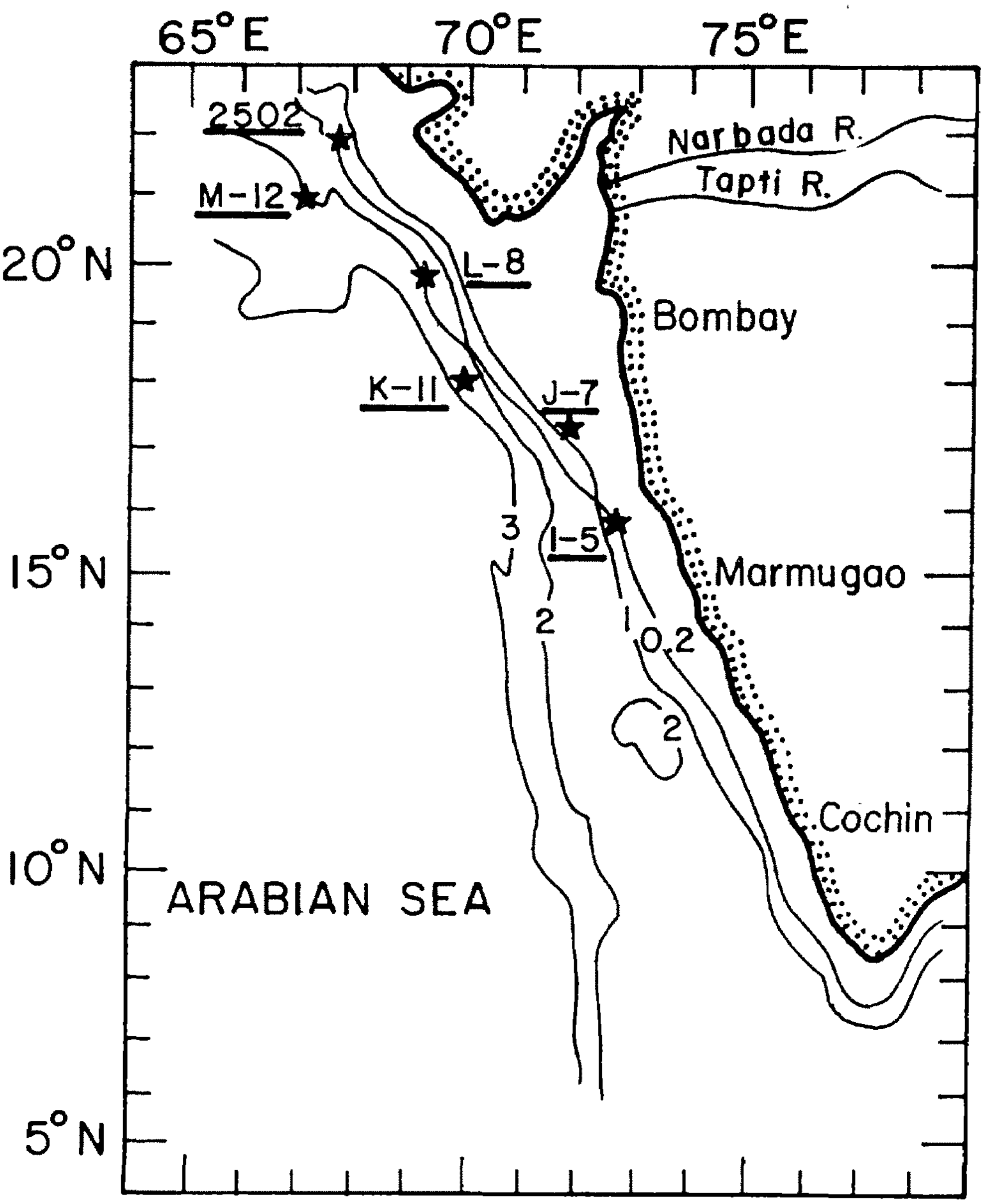

Fig. 2.1 Map showing core locations (⋆) along the WCMI with water-depth contours in km.

Table 2.1: Relevant details of sediment cores studied from the WCMI

Core	Location	Water depth (m)	Shipboard description
Upper slope			
L-8	$19^0 54' N, 69^0 24' E$	340 m	Light and green-grey clayey material H_2S smell below ~5 cm depth
J-7	$17^0 16' N, 71^0 47' E$	350 m	Coarse grained sediment with calcareous ooze and H_2S smell below ~5 cm depth
I-5	$15^0 23' N, 72^0 50' E$	350 m	Dark brown sand/silt with calcareous ooze
2502	$21^0 52' N, 68^0 E$	280 m	Brownish clayey material
Lower slope			
K-11	$18^0 01' N, 70^0 E$	2640 m	Light to dark brown clay material
M-12	$21^0 N, 67^0 E$	2300 m	Coarse grained brownish sediment

2.2 Chemical and isotopic measurements

In the laboratory, samples were dried at 110^{0}C for 10−12 h and were analyzed for $CaCO_3$, LOI (loss on ignition, an index for organic matter), radionuclides (^{238}U, ^{232}Th, ^{230}Th, ^{226}Ra, ^{210}Pb), major and trace elements (Fe, Al, Mn, Cu, Ni, Zn and Pb). A brief description of the analytical procedures employed for these measurements is given below.

(i) $CaCO_3$ and LOI measurements:

About 100 mg of the powdered sediment sample was repeatedly leached with 10 ml of 2% acetic acid (v/v). After each leaching, the slurry was centrifuged and supernate solution was collected and made to 50 ml. An aliquot of this solution was analyzed for Ca by the EDTA titration method using solochrome blackT as the indicator (Bassett et al,1978). Along with the samples, a number of standard solutions made from anhydrous $CaCO_3$ were also analyzed. Based on these analyses, $CaCO_3$ content of the samples was calculated. Samples in duplicate were also analyzed to check the reproducibility of the measurements. The weight loss on ignition (LOI) has been used as an index of organic matter. This was ascertained from the weight loss by heating ~1.0 g of dry, powdered sediment sample in air at 400^0C for 6–8 h.

(ii) Radionuclide measurements:

A number of nuclides belonging to the U–Th series (^{238}U, ^{234}U, ^{232}Th, ^{230}Th, ^{226}Ra and ^{210}Pb) were measured in the various sections of the sediment cores. Their distribution provides information on sediment accumulation rates, prevailing redox conditions and deposition of detrital and authigenic phases. These measurements were made following the standard radiochemical procedures (Krishnaswami and Sarin, 1976; Sarin et al 1979,1992). Briefly, ~ 2–3 g powdered sample was brought into solution by HF–$HClO_4$–HNO_3–HCl treatment in presence of ^{209}Po and ^{232}U–^{228}Th yield tracers.

The sample solution was finally converted in 0.5–0.6N HCl (~100 ml), to which ~50 mg of ascorbic acid was added in order to complex Fe^{3+}. From this solution, the Po isotopes (^{209}Po,^{210}Po) were autoplated onto a silver disc suspended in solution at a constant temperature of ~ 70^0C for 3h (Yadav et al,1992). The activities of the Po isotopes on the Ag disc were assayed by α-counting using a Si surface-barrier detector coupled to a pulse-height analyzer. The specific activity of ^{210}Pb in sediments was calculated from the measured activity of ^{210}Po.

After the Po plating, the solution was dried, residue digested with HNO_3 and dissolved in 9N HCl medium for further radiochemical separation (Fig.2.2). Uranium and thorium isotopes were separated from the solution and purified on an anion exchange column (AG1×8 Resin 100–200 mesh, Cl- form). The purified U and Th separates were then electroplated onto platinum planchets and assayed by α-spectrometry (Krishnaswami and Sarin,1976; Sarin et al,1992).

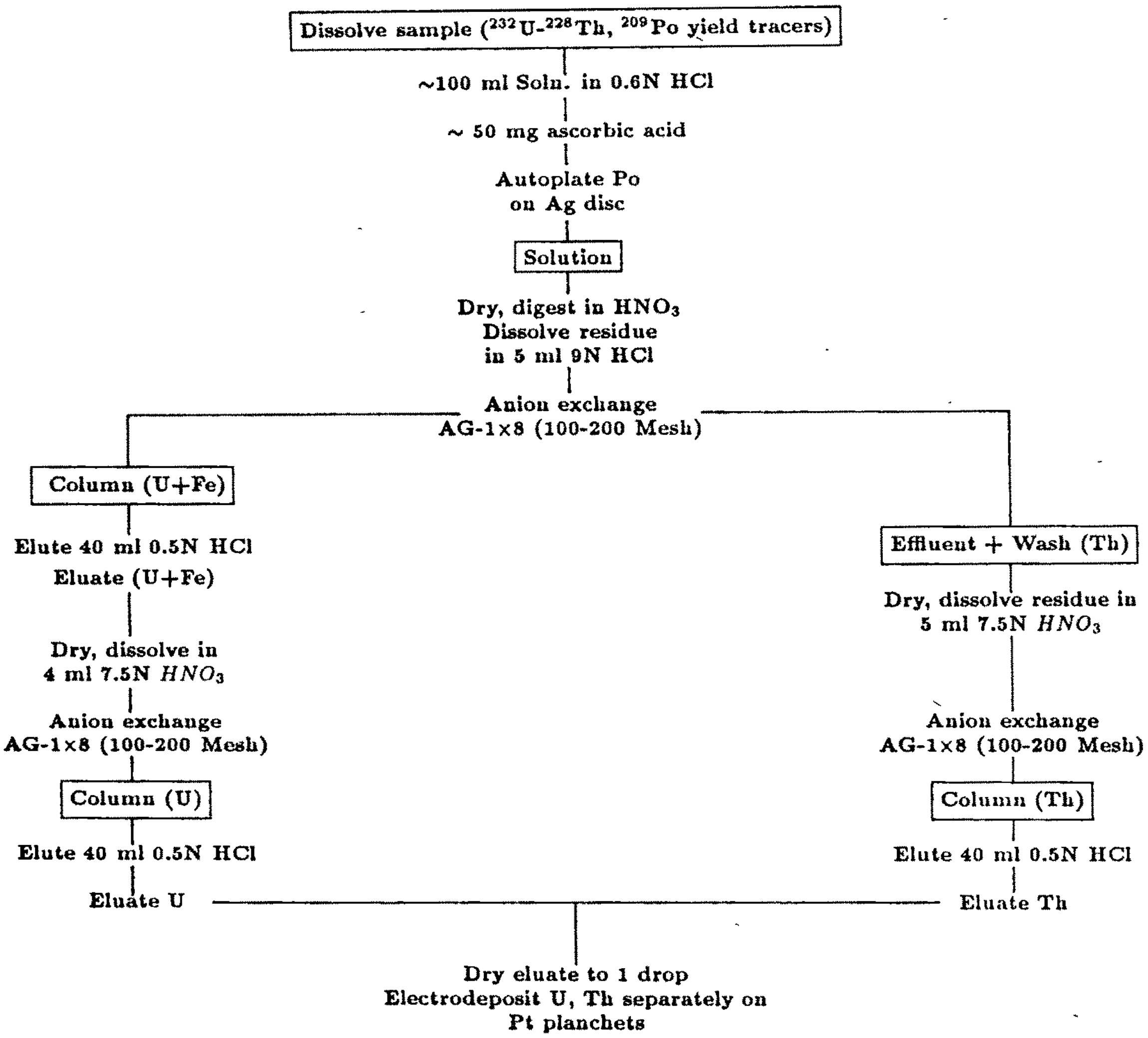

Fig. 2.2 Flow chart of the analytical procedure for separation of U, Th and Po isotopes from sediment samples (Sarin et al,1992).

For calculating the ^{232}Th and ^{230}Th concentrations, it was assumed that ^{232}Th and ^{228}Th are in radioactive equilibrium in the samples. This assumption may not be strictly valid in surface section of the cores, as there could be diffusional loss of ^{228}Ra and scavenging of ^{228}Th from bottom waters. However, as the activity of ^{228}Th tracer added as a yield monitor is 5–10 times the inherent ^{228}Th concentration, small departure from radioactive equilibrium (± 25%) between ^{228}Th and ^{232}Th would not significantly alter the ^{232}Th and ^{230}Th concentrations calculated assuming $^{232}\text{Th} \equiv {}^{228}\text{Th}$. To check on this two sediment samples [J-7(2–4 cm) and L-8(2–4 cm)] from upper slope region were processed for Th isotopes with and without spike. The calculated ratio of $^{228}Th/^{232}Th$ based on these analyses (Table 2.2) show that small departures in $^{228}Th/^{232}Th$ equilibrium do not affect the measured ^{230}Th and ^{232}Th concentrations. The replicate measurements of the U–Th nuclides in the samples indicate reproducibility of the results better than ±2 %.

Table 2.2 : Thorium measurements to check validity of assumption, $^{228}Th \equiv {}^{232}Th$.

Section	$^{228}Th/^{232}Th$	
	(a)	(b)
J-7 (2–4)	1.29±.04	10.29±.31
L-8 (2–4)	1.04±0.04	6.08±.21

(a) based on measurement in unspiked sample
(b) based on measurement in spiked sample

A separate aliquot of ~0.5 g dry powdered sediment sample was brought into solution by the HF–HClO$_4$–HNO$_3$–HCl treatment. The solution was transferred to a Rn measuring flask and purged with He gas and stored for the growth of ^{222}Rn. After about 2–3 weeks, the ^{222}Rn grown in from ^{226}Ra was milked and its activity assayed using scintillation counters (Mathieu,1988). The efficiency of extraction and counting was determined using ^{226}Ra standards. The standards and blanks were run periodically to check on the extraction efficiency and system characteristics.

The errors given in radionuclide concentrations are $\pm 1\sigma$ uncertainties calculated by appropriately summing the errors from counting statistics, blank corrections, and tracer calibrations. Blank runs for U ($^{238,234}U$) and Th ($^{232,230}Th$) showed activity levels < 1% of the signal values.

(iii) Major and Trace elements:

~0.5 g dry powdered sediment sample was brought into solution by digesting with HF–HClO$_4$–HNO$_3$–HCl treatment and made to 50 ml. The concentrations of Al, Ca, Fe, Mn, Ni, Cu, Zn and Pb were measured by Atomic Absorption Spectrophotometry (AAS) (Sarin et al,1979). The accuracy of measurements was checked by measuring these elements in USGS rock standards W-1 and G-2. The results are listed in Table 2.3 which show that the agreement between reported values (Flanagan,1973) and those measured in this study is reasonably good, except for Ni and Pb for which our values are significantly higher. The higher values result from molecular absorption which were not corrected using the deuterium background corrector. However, these values are not expected to affect the relative distribution of metal abundances in various sediment sections.

Table 2.3 : Results of analysis of USGS rock standards W-1 and G-2

Elements	Flanagan (1973)	Present work*
USGS-W1		
Na (%)	1.57	1.56±0.07
K (%)	0.5–0.55	0.50±0.03
Ca (%)	7.81–8.10	7.96±0.13
Mg (%)	4.0–4.05	3.82±0.14
Fe (%)	7.60–7.77	7.72±0.14
Al (%)	7.86	7.90±0.06
Cu (ppm)	112–121.5	119±0.2
Zn (ppm)	69–80	87.5±3
Ni (ppm)	70–90	91.0±2
Mn (ppm)	1254–1394	1372±23
USGS-G2		
Ca (%)	1.39–1.54	1.43
Pb (ppm)	31.2	53.1

* Errors given are ± 1σ based on repeat analyses. For Ca and Pb, in USGS-G2 no errors are given as they are based on a single measurement.

Another approach to obtain precision of the various parameters measured in this study is made through the calculation of the coefficient of variation using the following formula

(Brewer et al,1976).

$$C.V. = \sqrt{\frac{\Sigma(d_i/x_i)^2}{2n}} \times 100 \qquad (2.1)$$

where d_i is the difference in concentration between duplicates with their mean x, and n is the total sets of duplicate samples covering a wide range of concentrations. The repeat measurements showed reproducibility better than ±5% for $CaCO_3$ content in the range of 32 to 71%. The C.V. for different elements for the measured range of their concentrations are: Al 2%, Fe 4%, Ca 2%, Mn 2%, Ni 6%, Cu 5%, Zn 2% and Pb 7%.

The application of the radionuclide measurements and those of the major and trace elements to address the goals of the thesis are discussed in the next chapter.

Chapter 3

Results and Discussion

The spatial and temporal variations in the depositional fluxes of redox sensitive and particle reactive elements viz. U, Mn, ^{210}Pb and ^{230}Th have been studied along the WCMI. These data have been used for delineating the role of margin sediments in regulating their marine geochemical balance. In addition, temporal variations in the depositional fluxes of various elements will provide information on the environmental history of the region. To achieve some of these goals, the chronology of the sediments is very essential. This has been established by the ^{210}Pb method. For the lower slope cores an attempt has also been made to determine the sediment accumulation rate based on the ^{230}Th measurement in surface sections. Results on the chemical and isotopic analyses have been compared between the upper and lower slope sediments to evaluate the differences in the depositional patterns of various elements and their causative factors.

3.1 Geochronology of sediments

Chemical scavenging of particle reactive nuclides such as ^{210}Pb from the water-column and its subsequent delivery to sediments provides a means for evaluating the chronology of sediments. Towards this, it is necessary to ascertain the concentration of ^{210}Pb in sediments derived from the water-column, commonly termed as $^{210}Pb_{excess}$ or unsupported ^{210}Pb. In ^{210}Pb geochronology, the total ^{210}Pb content of sediments is considered to be made up of two components, ^{210}Pb derived from the water-column and ^{210}Pb continually being produced in the sediments from the decay of ^{226}Ra. The activity of $^{210}Pb_{excess}$ in sediment section is estimated from the relation:

$$^{210}Pb_{excess} = ^{210}Pb_{total} - ^{210}Pb_{supported} \tag{3.1}$$

where $^{210}\mathrm{Pb}_{total}$ is the total ^{210}Pb activity measured in the sample and $^{210}\mathrm{Pb}_{supported}$ is the ^{210}Pb activity in radioactive equilibrium with ^{226}Ra. The two basic assumptions involved in the ^{210}Pb based geochronology are: (a) the flux of ^{210}Pb to the sediment has remained unchanged and (b) no migration of this radionuclide has taken place over the dating interval. If these assumptions hold good, then for steady state, the ^{210}Pb concentration at any depth in the sedimentary column would be governed by particle mixing, sedimentation, radioactive decay, and its production from ^{226}Ra. The equation governing ^{210}Pb distribution (Goldberg and Koide, 1962; Nozaki et al,1977; Krishnaswami and Lal,1978) is:

$$\frac{\partial}{\partial z}\left(D\frac{\partial(\rho A)}{\partial z}\right) - S\frac{\partial(\rho A)}{\partial z} + \lambda P\rho - \lambda(\rho A) = \frac{\partial(\rho A)}{\partial t} \tag{3.2}$$

Where D is the particle mixing coefficient (cm^2/time), S is the sediment accumulation rate (cm/time), A is the specific activity of ^{210}Pb (dpm/g) and ρ is the in-situ density of sediment (g/cm^3). Eqn. (3.2) is a generalized form and allows for variation in mixing coefficient and density with depth. However, more commonly, D and ρ are assumed constant and system is considered to be in steady state, $\frac{\partial(\rho A)}{\partial t} = 0$. In shelf and margin sediments estimates of D can be derived by measuring ^{234}Th (Aller and Cochran,1976; Aller et al, 1980; Aller and DeMaster,1984) and/or fall-out nuclides e.g. ^{137}Cs and ^{239,240}Pu (Guinasso and Schink,1975). In the present study, attempts to derive information on particle mixing through measurement of ^{234}Th (Aller and Cochran,1976; Aller and DeMaster,1984) were not successful because of the long time delay between sampling and laboratory measurements. Since the upper slope sediments are from regions of anoxic or sub-oxic environments, biological activities leading to particle mixing is expected to be insignificant. Under these conditions, it has been assumed that D=0, i.e. no particle mixing occurs in the upper slope sediments. However, the importance of sediment mixing resulting from physical processes is difficult to assess.

With D=0, constant ρ and $\frac{\partial(\rho A)}{\partial t} = 0$, eqn. (3.2) reduces to:

$$\rho\left[-S\frac{\partial A}{\partial z}+\lambda P-\lambda A\right]=0 \tag{3.3}$$

Setting boundary condition, $A = A_0$ at z = 0, the solution of eqn. (3.3) is,

$$(A-P)=(A_0-P)_o\cdot e^{\left(-\frac{\lambda}{S}\right)\cdot z}$$

$$or,\quad (A_{210}-A_{226})=(A_{210}-A_{226})_o\cdot e^{\left(-\frac{\lambda}{S}\right)\cdot z} \tag{3.4}$$

$$or,\quad {}^{210}Pb_{excess}=({}^{210}Pb_{excess})_o\cdot e^{\left(-\frac{\lambda}{S}\right)\cdot z} \tag{3.5}$$

Where A_{210} and A_{226} are the activities (dpm/g) of ^{210}Pb and ^{226}Ra nuclides respectively and $(A_{210} - A_{226})_0$ is the $^{210}Pb_{excess}$ activity at surface z=0.

The assumption of constant ρ is supported by the observation that it does not show significant downcore variations (except the core M-12) as calculated from the $CaCO_3$−density relationship (Lyle and Dymond,1976). In the upper slope region, for the core J-7, uniform density of 0.58 g/cm^3 has been found throughout the core length, for L-8 it ranges from 0.42 to 0.51 g/cm^3 (mean = 0.44), for I-5 it ranges from 0.57 to 0.64 g/cm^3 (mean = 0.61) and for 2502 it ranges from 0.39 to 0.51 g/cm^3 (mean = 0.43). Similarly in lower slope region, the density of K-11 ranges from 0.42 to 0.51 g/cm^3 (mean = 0.47) and for the core M-12 it ranges from 0.29 to 0.43 g/cm^3 (mean = 0.33). The geometric mean of column averaged density of all the cores is 0.47. In all elemental flux calculations a value of 0.5 g/cm^3 for ρ has been used in this study.

To assess the validity of assumption that there is no particle mixing (i.e. D=0) in the upper slope sediments, ^{137}Cs ($t_{1/2}$=30.2 y) was measured in one of the cores, J-7, by non-destructive γ-ray spectrometry. The results are given in Table 3.1 and relative downcore variation of ^{137}Cs is presented in Fig. 3.1. The activity of ^{137}Cs could be detected to a depth of ~ 6 cm from the surface, with its peak in 4−5 cm depth section. The sediment accumulation rate for this core was calculated from the peak ^{137}Cs concentration which corresponds to 1963, the year of its maximum fallout (Pierson,1971; Pennington et al,1973; Delaune et al,1978; Hermanson,1990), and 1988, the year of sample collection. The calculated sediment accumulation rate of ~ 1.8 mm/y based on ^{137}Cs profile is same

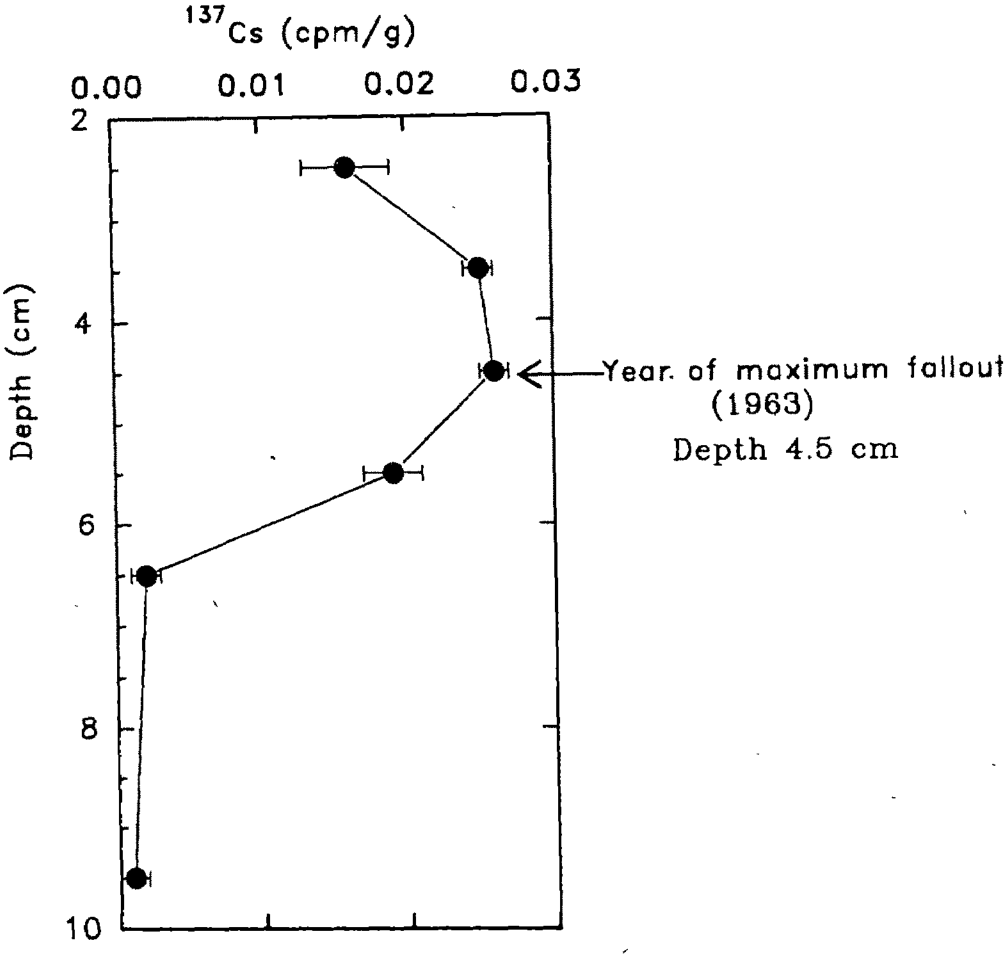

Figure 3.1: ^{137}Cs depth profile for the sediment core J-7

as that derived from the ^{210}Pb chronology as mentioned below. If the bioturbation effects are significant, then the activity of ^{137}Cs is expected further deep in the sediments, and hence the rate of sediment accumulation would be higher. As this is not observed in the core J-7, particle mixing due to bioturbation is ruled out. Therefore, assumption of D=0 (i.e no particle mixing) for these sediments in the upper slope which show smooth exponential decay of $^{210}Pb_{excess}$ is valid and hence eqn. (3.5) can be used for sediment chronology with a better degree of confidence.

Table 3.1: Distribution of ^{137}Cs in the sediment core J-7

Depth section (cm)	^{137}Cs (cpm/g)
(2–3)	0.016±0.003
(3–4)	0.025±0.001
(4–5)	0.026±0.001
(5–6)	0.019±0.002
(6–7)	0.002±0.001
(9–10)	0.001±0.001

Eqn. (3.5) predicts exponential decay of $^{210}\mathrm{Pb}_{excess}$ with depth. The $^{210}\mathrm{Pb}_{excess}$ vs. depth profiles for the upper slope sediments are given in Fig. 3.2. The depth profiles of all cores except 2502 show smooth exponential decay with depth which has been interpreted in terms of sediment accumulation and radioactive decay. The ^{210}Pb derived sediment accumulation rates range from 0.25 to 1.83 mm/y (Fig. 3.2) for the various cores. The activity of unsupported ^{210}Pb ($^{210}\mathrm{Pb}_{excess}$) in the surface (0–2 cm) section of the bulk sediments from upper slope region ranges from 10.6 to 31 dpm/g (Table 3.2), while the radium supported ^{210}Pb is ~0.7 dpm/g.

In core I-5, the $^{210}\mathrm{Pb}_{excess}$ activity decreases to very low values in the (4–6 cm) section itself. This makes it difficult to obtain an estimate of sediment accumulation in the core. However, the best fit line drawn through three data points (Fig. 3.2) yields a sediment accumulation rate of 0.39 mm/y for this core. The core 2502 shows an evidence of particle mixing in the surface as reflected by the near uniform activity of $^{210}\mathrm{Pb}_{excess}$ in the (0–7) cm interval from the surface (Fig.3.2). In this core, therefore, the sediment accumulation rate has been determined from the $^{210}\mathrm{Pb}_{excess}$ data in the depth interval (7–30cm) (Fig. 3.2). Assuming that the sediment accumulation rates based on $^{210}\mathrm{Pb}_{excess}$ in the cores to be same throughout the core length; the time span covered by the upper slope cores is estimated to be in the range of 100–800 years (J-7: 120 y; L-8: 800 y and I-5: 360 y).

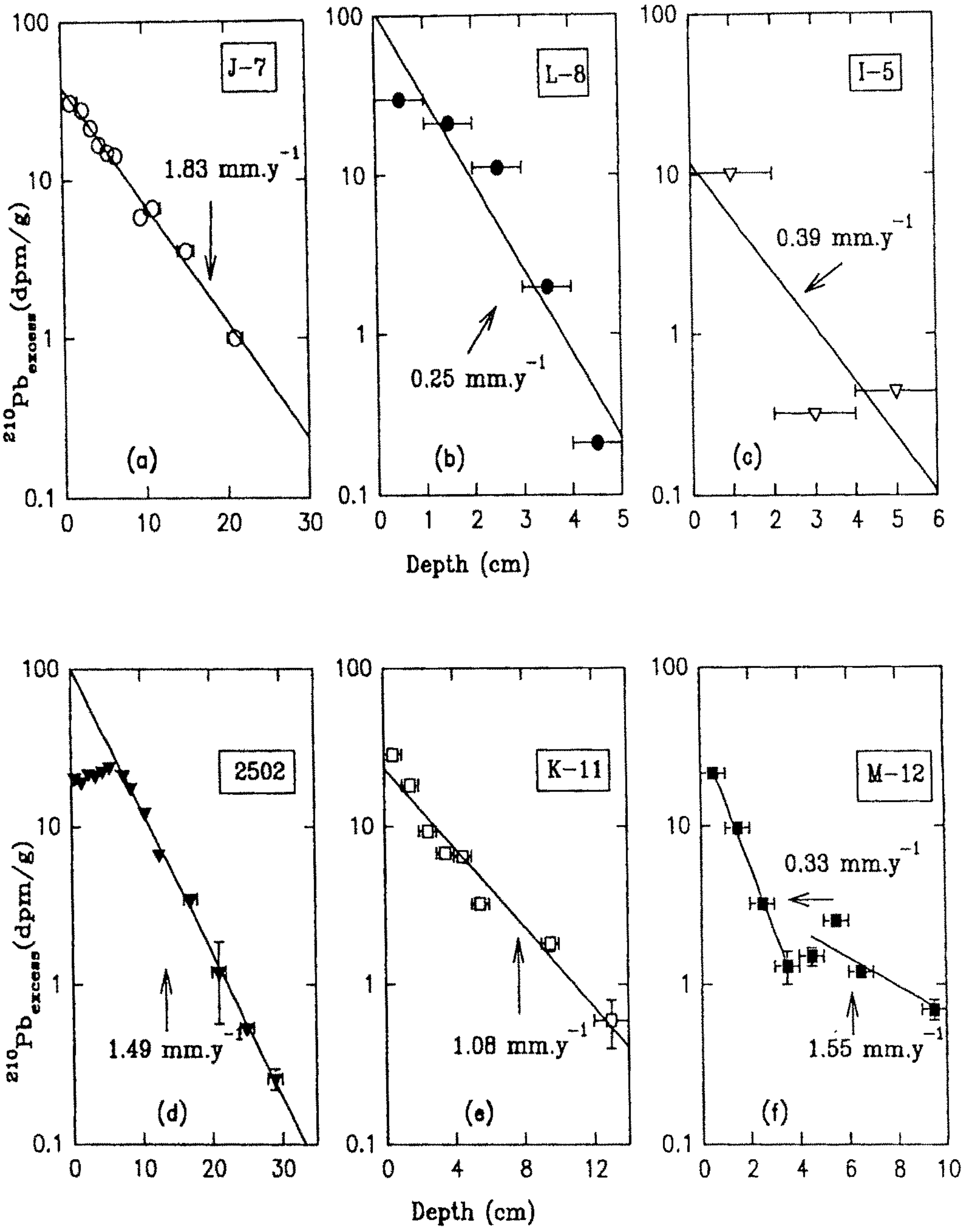

Figure 3.2: Concentration–depth profiles of $^{210}Pb_{excess}$ in sediment cores from the WCMI. The $^{210}Pb_{excess}$ distribution shows evidence of particle mixing in core 2502. In core M-12 there is a break in the slope at about 5 cm from the surface. The sediment accumulation rates of the cores, derived from the slope of the regression line are also given [eqn. (3.5)].

Table 3.2: $CaCO_3$ Concentration and Radionuclide Data† for the upper slope sediments

Sample Depth (cm)	$CaCO_3$ (%)	^{226}Ra ($dpm.g^{-1}$)	$^{210}Pb_{excess}$ ($dpm.g^{-1}$)	^{238}U ($dpm.g^{-1}$)	$^{234}U/^{238}U$	^{232}Th ($dpm.g^{-1}$)	^{230}Th ($dpm.g^{-1}$)
J-7							
(0-2)	67.4	0.71 ± 0.03	30.9 ± 0.8	4.45 ± 0.12	1.10 ± 0.02	0.34 ± 0.01	0.62 ± 0.02
(2-3)	65.3	0.57 ± 0.03	27.6 ± 0.5	4.98 ± 0.12	1.12 ± 0.01	0.34 ± 0.01	0.62 ± 0.02
(2-3)R	65.3	-	-	4.76 ± 0.17	1.15 ± 0.03	0.34 ± 0.02	0.63 ± 0.02
(3-4)	65.3	-	21.3 ± 0.6	5.19 ± 0.13	1.16 ± 0.01	0.42 ± 0.02	0.79 ± 0.03
(4-5)	71.4	-	16.7 ± 0.4	5.13 ± 0.13	1.11 ± 0.01	0.37 ± 0.01	0.71 ± 0.02
(5-6)	71.5	-	15.0 ± 0.3	4.97 ± 0.14	1.18 ± 0.02	0.39 ± 0.02	0.65 ± 0.03
(6-7)	67.3	0.67 ± 0.04	14.2 ± 0.3	5.10 ± 0.13	1.14 ± 0.02	0.39 ± 0.02	0.71 ± 0.02
(9-10)	72.1	0.67 ± 0.05	5.9 ± 0.2	-	-	-	-
(10-12)	67.9	-	6.7 ± 0.2	5.34 ± 0.13	1.13 ± 0.02	0.45 ± 0.02	0.76 ± 0.03
(14-16)	64.9	0.72 ± 0.04	3.6 ± 0.1	5.96 ± 0.15	1.12 ± 0.01	0.44 ± 0.02	0.69 ± 0.02
(18-20)	68.8	-	-	5.92 ± 0.14	1.12 ± 0.01	0.38 ± 0.01	0.70 ± 0.02
(20-22)	68.6	-	1.0 ± 0.05	5.94 ± 0.16	1.18 ± 0.02	0.40 ± 0.02	0.74 ± 0.04
L-8							
(0-1)	43.2	0.75 ± 0.03	29.9 ± 0.6	4.25 ± 0.11	1.09 ± 0.02	0.75 ± 0.04	0.96 ± 0.05
(1-2)	43.2	0.75 ± 0.03	21.2 ± 0.5	4.25 ± 0.11	1.11 ± 0.02	0.83 ± 0.03	0.94 ± 0.03
(2-3)	46.2	0.66 ± 0.03	11.2 ± 0.2	3.99 ± 0.09	1.13 ± 0.02	-	-
(3-4)	46.2	0.66 ± 0.03	2.0 ± 0.1	5.29 ± 0.14	1.13 ± 0.01	-	-
(2-4)	46.2	0.66 ± 0.03	-	5.88 ± 0.18	1.15 ± 0.02	0.72 ± 0.03	0.92 ± 0.04
(4-5)	46.7	-	0.21 ± 0.01	6.07 ± 0.19	1.13 ± 0.02	0.75 ± 0.03	0.99 ± 0.04
(5-6)	46.7	-	⋆	7.14 ± 0.19	1.10 ± 0.02	0.65 ± 0.02	0.82 ± 0.03
(6-7)	46.5	-	⋆	7.29 ± 0.17	1.14 ± 0.01	0.81 ± 0.02	1.04 ± 0.03
(18-20)	58.5	-	-	5.73 ± 0.18	1.13 ± 0.02	0.54 ± 0.02	0.77 ± 0.03

† concentration expressed on bulk sediment basis

R denotes repeat measurement

- indicates that measurements were not made

⋆ No measurable $^{210}Pb_{excess}$ observed.

Table 3.2 $CaCO_3$ Concentration and Radionuclide Data[†] for the upper slope sediments (CONTINUED)

Sample Depth (cm)	$CaCO_3$ (%)	^{226}Ra ($dpm.g^{-1}$)	$^{210}Pb_{excess}$ ($dpm.g^{-1}$)	^{238}U ($dpm.g^{-1}$)	$^{234}U/^{238}U$	^{232}Th ($dpm.g^{-1}$)	^{230}Th ($dpm.g^{-1}$)
I-5							
(0-2)	75.2	-	10.2 ± 0.2	1.03 ± 0.03	1.18 ± 0.02	0.26 ± 0.01	0.49 ± 0.02
(2-4)	74.0	-	0.32 ± 0.03	1.15 ± 0.03	1.13 ± 0.02	0.26 ± 0.01	0.52 ± 0.02
(4-6)	73.4	-	0.44 ±0.02	1.29 ± 0.03	1.14 ± 0.02	0.37 ± 0.02	0.66 ± 0.02
(6-8)	73.4	-	⋆	1.29 ± 0.03	1.14 ± 0.02	0.36 ± 0.02	0.68 ± 0.02
(8-10)	70.0	-	⋆	1.52 ± 0.04	1.10 ± 0.02	0.42 ± 0.02	0.79 ± 0.02
(10-12)	66.7	-	⋆	1.57 ± 0.04	1.11 ± 0.02	0.49 ± 0.02	0.82 ± 0.02
(12-14)	68.7	-	⋆	1.88 ± 0.05	1.12 ± 0.02	0.49 ± 0.02	0.84 ± 0.03
2502							
(0-1)	37.6	0.79 ± 0.04	20.31 ± 0.47	-	-	-	-
(1-2)	37.6	-	19.22 ± 0.56	-	-	-	-
(2-3)	40.5	-	21.71 ± 0.57	-	-	-	-
(3-4)	40.5	0.76 ± 0.04	21.23 ± 0.50	-	-	-	-
(4-5)	38.2	-	22.41± 0.63	-	-	-	-
(5-6)	38.2	-	24.07± 0.62	-	-	-	-
(7-8)	46.4	-	21.32± 0.52	-	-	-	-
(8-9)	40.5	-	17.61± 0.47	-	-	-	-
(10-11)	40.6	-	12.29± 0.35	-	-	-	-
(12-13)	49.0	-	6.66± 0.18	-	-	-	-
(16-18)	47.8	0.94±0.05	3.43±0.11	2.90±0.01	1.13±0.03	1.66±0.06	1.40±0.05
(20-22)	-	0.88±0.05	1.20±0.06	2.80±0.01	1.19±0.03	1.68±0.06	1.39±0.05
(24-26)	50.0	0.86±0.05	0.54±0.04	2.30±0.01	1.13±0.03	1.53±0.05	1.27±0.05
(28-30)	59.3	0.81±0.04	0.26±0.04	2.90±0.02	1.13±0.02	1.46±0.05	1.20±0.04

†concentration expressed on bulk sediment basis - indicates that measurements were not made

⋆ No measurable $^{210}Pb_{excess}$ observed.

Table 3.3 $CaCO_3$ concentration and Radionuclide Data[†] for the lower slope sediments

Depth (cm)	$CaCO_3$ (%)	^{226}Ra (dpm.g^{-1})	^{210}Pb$_{excess}$ (dpm.g^{-1})	^{238}U (dpm.g^{-1})	^{234}U/^{238}U	^{232}Th (dpm.g^{-1})	^{230}Th (dpm.g^{-1})
K-11							
(0-1)	43.9	3.86 ± 0.16	28.5 ± 0.6	0.78 ± 0.03	1.07 ± 0.04	0.88 ± 0.03	4.58 ± 0.12
(1-2)	49.2	-	18.1 ± 0.5	0.81 ± 0.03	1.04 ± 0.03	0.88 ± 0.03	4.53 ± 0.13
(2-3)	50.9	-	9.3 ± 0.3	0.81 ± 0.03	1.12 ± 0.04	0.87 ± 0.04	4.63 ± 0.14
(3-4)	51.2	-	6.7 ± 0.3	1.02 ± 0.03	0.99 ± 0.03	1.13 ± 0.04	4.84 ± 0.14
(4-5)	53.2	-	6.4 ± 0.3	0.92 ± 0.03	1.06 ± 0.03	1.00 ± 0.04	4.51 ± 0.14
(5-6)	51.6	6.0 ± 0.20	3.2 ± 0.3	1.04 ± 0.03	0.99 ± 0.02	1.05 ± 0.04	4.52 ± 0.14
(9-10)	54.6	-	1.8 ± 0.2	0.86 ± 0.03	1.05 ± 0.03	0.96 ± 0.03	4.18 ± 0.12
(12-14)	52.3	-	0.6 ± 0.2	0.92 ± 0.03	1.11 ± 0.03	0.87 ± 0.03	4.28 ± 0.11
(16-18)	56.3	2.60 ± 0.20	⋆	1.33 ± 0.05	1.09 ± 0.04	0.92 ± 0.03	3.63 ± 0.09
(18-20)	56.3	-	⋆	1.59 ± 0.04	1.08 ± 0.02	0.79 ± 0.03	2.99± 0.08
(22-24)	59.7	2.30±0.10	⋆	2.85 ± 0.08	1.09 ± 0.02	0.82 ± 0.03	3.01 ± 0.08
M-12							
(0-1)	18.2	5.80 ± 0.20	21.5 ± 0.6	1.26 ± 0.04	1.03 ± 0.03	2.78 ± 0.08	2.88 ± 0.08
(1-2)	18.2	6.50 ± 0.10	9.7 ± 0.4	1.25 ± 0.04	1.02 ± 0.03	2.58 ± 0.08	2.49 ± 0.08
(2-3)	23.2	3.30 ± 0.20	3.2 ± 0.3	1.25 ± 0.04	1.09 ± 0.03	2.29 ± 0.08	2.24 ± 0.08
(3-4)	23.2	3.10 ± 0.10	1.3 ± 0.3	1.47 ± 0.05	1.03 ± 0.03	2.10 ± 0.07	2.24 ± 0.07
(4-5)	27.4	3.20 ± 0.20	1.5 ± 0.2	1.44 ± 0.05	1.09 ± 0.03	2.19 ± 0.07	2.34 ± 0.08
(5-6)	-	3.70 ±0.10	2.5 ± 0.2	-	-	-	-
(6-7)	31.6	4.00 ±0.10	1.2 ±0.1	1.36 ± 0.04	1.06 ± 0.03	1.65 ± 0.05	2.95 ± 0.08
(9-10)	-	4.00 ± 0.10	0.7 ± 0.1	-	-	-	-
(12-14)	36.9	-	⋆	1.37 ± 0.04	1.08 ± 0.03	1.44 ± 0.04	3.02 ± 0.08
(20-25)	45.0	-	⋆	2.25 ± 0.06	1.08 ± 0.02	1.26 ± 0.04	2.98 ± 0.08

[†] concentration expressed on bulk sediment basis

- indicates that measurements were not made

⋆ No measurable $^{210}Pb_{excess}$ observed

For the two lower slope sediments cores (K-11 & M-12), because of the oxic conditions at the sediment-water interface, bioturbation cannot be ruled out. Therefore, for these two cores the sediment accumulation rates based on $^{210}\mathrm{Pb}_{excess}$ decay (1.08 and 0.33 mm/y respectively for K-11 and M-12, Fig. 3.2) could be an upper limit. The $^{210}\mathrm{Pb}_{excess}$ activity in surface section of K-11 and M-12 sediment cores (Table 3.3) is, 28.5 and 21.5 dpm/g respectively. The $^{210}\mathrm{Pb}_{excess}$ versus depth profile for M-12 (Fig. 3.2) shows two distinct slopes indicating a change in sediment accumulation rate. The deeper sections (> 5 cm from surface) of the core have higher rate of sediment accumulation (1.55 mm/y) than that in the surface ~ 5 cm (0.33 mm/y).

An independent approach to determine the rate of sediment accumulation for the cores from the lower slope region is based on the measured concentration of $^{230}\mathrm{Th}_{excess}$ activity (dpm/g) in their surface sections and comparing it with the ^{230}Th production rate from the overlying water-column. Analogous to ^{210}Pb, ^{230}Th content of sediments is also made of two components; one scavenged from seawater and the other continentally derived. The total activity of ^{230}Th in a sediment section, as measured by totally dissolving the sample, can be expressed as:

$$^{230}Th_{total} = ^{230}Th_{excess} + ^{230}Th_{detrital} \tag{3.6}$$

where $^{230}\mathrm{Th}_{detrital}$ is the continentally derived component. One approach to obtain $^{230}\mathrm{Th}_{detrital}$ component of sediments would be to assume that ^{238}U and ^{230}Th are in radioactive equilibrium. This may not be a quantitative approach as in the river suspended phases ^{230}Th is generally in excess of uranium (Scott,1982; Sarin et al,1990). Therefore, a better approach to assess the detrital contribution is from a knowledge of the $^{230}\mathrm{Th}/^{232}\mathrm{Th}$ ratios in river sediments draining into the margin. The Narbada, Tapi and the Indus are the rivers supplying sediments to the eastern Arabian sea, however, there is no data on the $^{230}\mathrm{Th}/^{232}\mathrm{Th}$ ratios of these sediments. In the absence of such data the activity of $^{230}\mathrm{Th}_{detrital}$ was estimated using the relation:

$$^{230}Th_{detrital} = \left(\frac{^{230}Th}{^{232}Th}\right)_{upper\ slope} \cdot {}^{232}Th_{lower\ slope} \tag{3.7}$$

This approach assumes that the $^{230}\mathrm{Th}/^{232}\mathrm{Th}$ of upper slope sediments is representative of the detrital component. This assumption should be valid as these cores are from very shallow water depths and hence the deposition of ^{230}Th from the overlying water column would be insignificant unless there is boundary scavenging and focusing of ^{230}Th.

Using the average ^{230}Th/^{232}Th activity ratio of (1.64 ±0.24) for L-8, J-7 and I-5 cores and ^{232}Th (0.88±0.03 dpm/g) measured in the upper section of the core K-11, $^{230}\mathrm{Th}_{detrital}$ is calculated to be 1.44±0.39 dpm/g. From the $^{230}\mathrm{Th}_{total}$ (4.58±0.12 dpm/g), $^{230}\mathrm{Th}_{excess}$ activity of 3.14±0.41 dpm/g is estimated for the core K-11. The $^{230}Th_{excess}$ activity in surface section is related to the ^{230}Th depositional flux and sediment accumulation rate (Krishnaswami,1976) as:

$$A_0^{230} = \frac{F}{S \cdot \rho} \tag{3.8}$$

where $A_0{}^{230}$ is the $^{230}Th_{excess}$ activity at the core top (dpm/g), F is the depositional flux of ^{230}Th, i.e. equivalent to its production rate from ^{234}U in the water column, S the sediment accumulation rate and ρ is the density of sediment. The value of F for K-11 (water depth 2600 m) is 6.8 dpm/cm^2 ·10^3 y. Using $\rho = 0.5$ g/cm^3 and $A_0^{230} = 3.14 \pm 0.41$ dpm/g, the sediment accumulation rate for the core is calculated to be 0.04 mm/y. This rate is about an order of magnitude lower than that derived from the $^{210}\mathrm{Pb}_{excess}$ profile. If the $^{230}\mathrm{Th}_{excess}$ based sediment accumulation rate is indeed valid then it would imply that the $^{210}\mathrm{Pb}_{excess}$ distribution in this core is considerably influenced by particle mixing. Alternately, the high $^{230}\mathrm{Th}_{excess}$ in the surface sediments could result from focussing and boundary scavenging effects (Anderson et al, 1983). Therefore, the above mentioned $^{230}\mathrm{Th}_{excess}$ method of dating the sediments can be questionable. Attempt to use similar approach for deriving sediment accumulation rate in the core M-12 was not successful, as the (^{230}Th/^{232}Th) activity ratio in its surface section is comparable to or less than the mean ratio (1.64 ±0.24) in the upper slope sediments.

^{14}C chronology

In addition to ^{210}Pb and ^{230}Th nuclides, attempts were also made to determine the ages of these sediments using ^{14}C as these sediments are calcareous (18–75% $CaCO_3$). The ^{14}C measurements were made at the PRL (Chemistry) Radiocarbon laboratory (Bhushan et al,1994). The ^{14}C ages of various sections in core J-7 center around 7200 years; whereas in the core M-12, the ^{14}C ages show a reversal with the oldest age at the surface compared to that for the deeper sections (Table 3.4). For the core K-11, the ^{14}C age increases from 3780±70 y in the (5−10) cm section to 7640±70 y in the (20−22.5) cm section (R. Bhushan, Personal communication). Prior to this work, ^{14}C ages for surficial sediments and limestone formations along the western shelf of India have been reported to be ranging from 11000 to 9000 years B.P. (Nair,1975; Nair et al,1979; Rao et al,1994).

The ^{14}C data obtained in this study can be explained based on the occurrence of relict calcareous materials such as oolitic and algal limestones and calcareous sand stones along the WCMI (Rao,1978; Nair and Hashimi,1980; Rao et al, 1994). Also, there is possibility of dead calcareous material from the milliolite deposits which are abundantly present in Saurashtra coast (Baskaran,1985). The mixing of these relict carbonates with nascent carbonate shells settling from the water column can yield older ages measured in this work. Unless the effect of mixing of various carbonates is ascertained it is not possible to obtain reliable ages based on ^{14}C. Therefore, the ^{14}C data have not been used to derive sediment accumulation rates.

Table 3.4: ^{14}C ages of WCMI sediments

Depth (cm)	Age B.P. (y)
J-7	
(0-4)	7100±85
(6-10)	7485±64
(24-29)	7093±62
M-12	
(0-4)	6323±106
(14-16)	4308±71
(20-25)	4623±76
K-11	
(5-10)	3786±70
(15-20)	7000±67
(20-22.5)	7641±72

3.2 $CaCO_3$ and Organic matter

The occurrence of both $CaCO_3$ and organic matter in sediments is biogenic in nature, their abundances are in some way related to the overhead water-column productivity. The abundance of $CaCO_3$ in upper slope sediments, along 350 m bathymetry over 5^0 latitudinal distance (20–15^0N), shows significant spatial variation. In cores J-7, L-8, I-5 and 2502, $CaCO_3$ content ranges from 37 to 75% (Table 3.2, Fig. 3.3). Within each of these cores there is no significant downcore variations. The calculated mean $CaCO_3$ abundance, along with the standard deviation in each core is: J-7 (68.6±2.7%), L-8 (47.7±4.3%), I-5 (73.9±0.8%) and 2502 (43.5±6.5%).

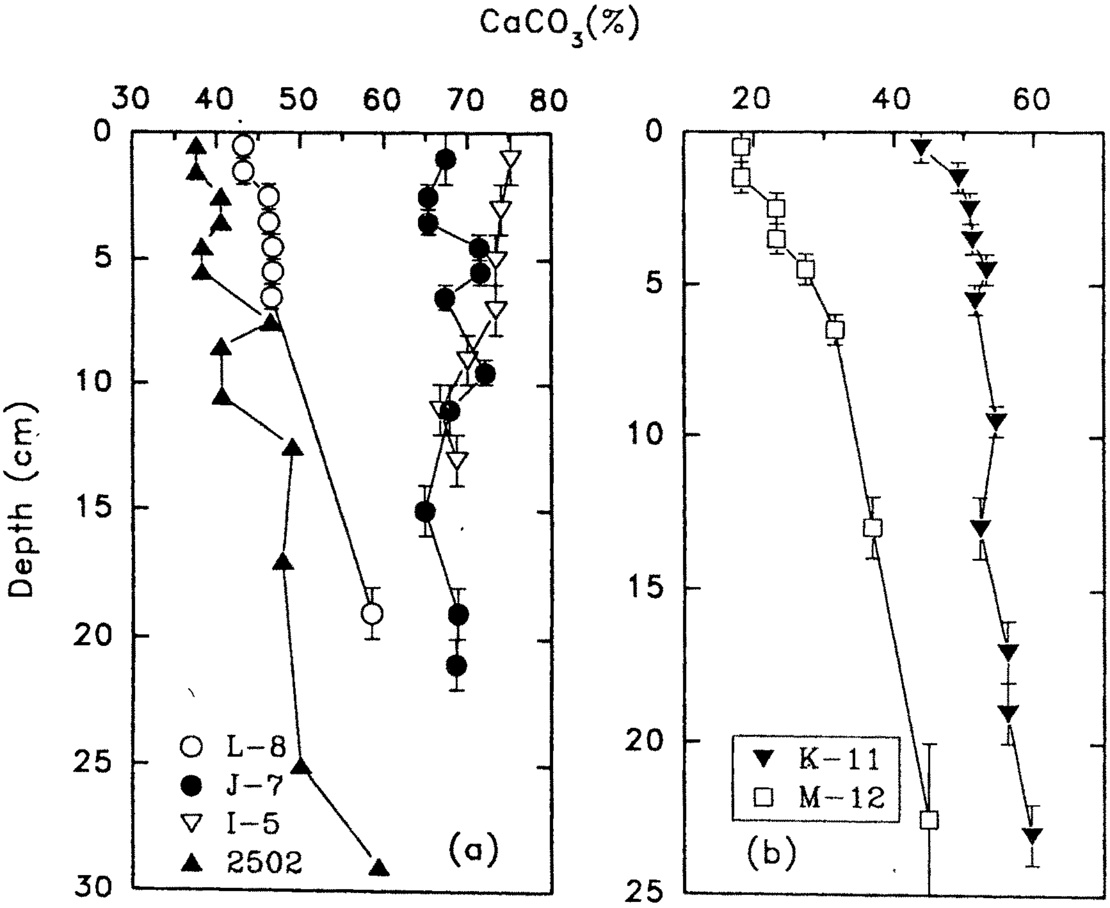

Figure 3.3: Variation in $CaCO_3$ content with depth for (a) upper and (b) lower slope sediments respectively.

The observed range in $CaCO_3$ abundances agrees well with the values reported in earlier studies (Rao,1978; Kolla et al,1981; Borole et al,1982a) for this region. Use of $CaCO_3$ content in sediments as a measure of paleoproductivity requires that the $CaCO_3$

in the sediments is solely derived from the biological productivity in the water column and that they are well preserved after deposition. This condition is, however, may not strictly valid for the WCMI sediments as they may have relict carbonates; as evidenced from the "older" ^{14}C ages of these carbonate sediments. Because of this, the $CaCO_3$ content of these sediments has not been used as a proxy for productivity. It is also noteworthy that $CaCO_3$ increases southward from 20^0N latitude, which has been attributed to enhanced biological production based on foraminiferal analysis (Naidu et al, 1992).

The content of organic matter (as inferred from loss in weight on ignition) decreases from 15% to 3% between 20 to 17^0N along the same 350 m bathymetry. The highest organic matter in surface sediments has been found in the core L-8 (15%) followed by that in the core J-7 (7.7%). These cores are essentially from anoxic regions (as evidenced by H_2S smell during sampling) where better preservation of organic matter is expected. Earlier study (Paropkari et al,1992) has shown that the organic matter in upper slope region is primarily of marine origin and is derived from productivity of overlying waters which varies from 0.25 to 0.75 $gC/m^2{\cdot}d$. This range of productivity is nearly three times lower than that from other coastal regions of the Arabian sea. Also, moderate to high concentrations of organic carbon (2–4 and 4–16%) are reported over the entire upper slope region (Kolla et al,1981; Paropkari et al,1992). High organic carbon observed in this region is generally interpreted in terms of its efficient preservation under anoxic conditions (Kolla et al,1981; Paropkari et al,1992) which depends primarily on the high rate of sediment accumulation.

The calcium carbonate content in the sediment cores, K-11 and M-12, from the lower slope region ranges from 18 to 60% respectively. M-12 shows the lowest calcium carbonate concentration compared to all other cores analyzed in the present study. These values of $CaCO_3$ are again consistent with the previous studies (Kolla et al,1981). In both the lower slope cores, a systematic increase in $CaCO_3$ content with depth is observed (Fig. 3.3). Maximum $CaCO_3$ variation, to an extent of 60% relative to the surface, is seen in the core M-12. Such a change can result from temporal variation in depositional environment. An alternative interpretation for the downcore increase in $CaCO_3$ in these cores can be sought as due to the deposition of $CaCO_3$ (relative to detrital silicate) being higher in the past compared to that at the present. Nair and Hashimi (1981) have reported an increased deposition of relict calcareous materilas during the Holocene period along the western continental shelf which might have also influenced the deeper section of the lower slope cores. The contribution of relict carbonates to various depth needs to be ascertained to use the $CaCO_3$ depositional flux as an index of paleoproductivity. The content of organic matter in both the lower slope cores is about 3% in their surface sections. A marked difference in organic matter contents between upper and lower slope sediments could be attributed to their combustion through the water column.

3.3 ^{210}Pb depositional flux

The $^{210}Pb_{excess}$ inventory and depositional flux provide information about the importance of overhead vs. boundary scavenging processes at the core sites (Bacon et al,1976; Spencer et al,1981; Cochran et al, 1983; Thomson et al,1993).

Inventories of $^{210}Pb_{excess}$ in the margin sediments can be calculated using the relation:

$$\mathrm{I} = \rho \cdot \int_0^\infty \mathrm{A(z)dz} \tag{3.9}$$

$$\text{or,}\ \mathrm{I} = \rho \cdot \Sigma(\mathrm{A_i.z_i}) \tag{3.10}$$

and is related to the mean ^{210}Pb depositional flux by:

$$\mathrm{J} = \lambda_{210}.\mathrm{I} \tag{3.11}$$

where I is the $^{210}Pb_{excess}$ inventory,in dpm/cm^2; ρ is the *in-situ* density of sediments (0.5 g/cm^3), z_i is the thickness of sample in cm at depth interval i; J is the mean $^{210}Pb_{excess}$ depositional flux at the core site in dpm/cm^2·y and λ_{210} is the ^{210}Pb decay constant(0.0311 y^{-1}). For the cores analyzed in this study, the calculated *in-situ* density ρ based on Lyle and Dymond (1976), ranges between 0.29 to 0.64 g/cm^3 and is fairly constant with depth with an exception of the core M-12. The assumption of constant density of 0.5 g/cm^3 is not strictly valid for the core M-12 where it increases with depth from 0.29 to 0.43 g/cm^3. The average density ($\overline{\rho}$) calculated for each core is given in Table 3.5, however, a value of 0.5 g/cm^3 is used for the calculation of I. The calculated values of the $^{210}Pb_{excess}$ inventory for the different cores are given Table 3.5 along with the sediment accumulation rates and extrapolated $^{210}Pb_{excess}$ activities (i.e. A_o) at sediment-water interface. The value based on eqn. (3.10) is a better estimation of $^{210}Pb_{excess}$ inventory, as this represents the sum of measured $^{210}Pb_{excess}$ activities in the sediment column. Also in cores such as M-12, this method of finding the $^{210}Pb_{excess}$ inventory is logical as the sediment accumulation has changed with depth.

Table 3.5: Rates of sediment accumulation and $^{210}Pb_{excess}$ inventory in WCMI sediments

Core	$\bar{\rho}$ (g/cm^3)	S (mm/y)	A_0 (dpm/g)	I* (dpm/cm^2)	$J_{obs.}$ (dpm/cm^2·y)	$J_{exp.}$ (dpm/cm^2·y)
J-7	0.58	1.83	38.5	108.7	3.38	1.1
L-8	0.44	0.25	107.2	31.8	0.99	1.1
I-5	0.61	0.39	11.9	10.9	0.34	1.1
2502	0.43	1.49	100.0	133.1	4.14	1.1
K-11	0.47	1.08	28.4	41.5	1.29	1.85
M-12	0.33	0.33, 1.55	36.5	20.6	0.64	1.85

* based on eqn. (3.10)

Using eqn.(3.10), the calculated mean depositional flux of $^{210}Pb_{excess}$ in sediments from upper slope region (J-7, L-8, I-5 and 2502) ranges between 0.34 to 4.14 dpm/cm^2·y (Table 3.5). Since these sediment cores are from the region of water depth ranging between 280 to 350 m, the $^{210}Pb_{excess}$ flux derived from its *in-situ* production (from ^{226}Ra, typically 0.1 dpm/l; Sarin et al,1994) in the water column would be ~ 0.1 dpm/cm^2·y, which is, around 10% of atmospheric fallout (~ 1 dpm/cm^2·y; Lal et al,1979). Therefore, $J_{exp.}$ flux would be 1.1 dpm/cm^2·y (Table 3.5) of which the dominant component is from the atmospheric fallout. For the two cores from the lower slope region (K-11 and M-12), in addition to atmospheric supply, the ^{210}Pb flux of 0.85 dpm/cm^2·y (Sarin et al,1992) from overlying water-column (based on $^{210}Pb—^{226}Ra$ disequilibrium) also contributes to the total ^{210}Pb inventory. Therefore, the ^{210}Pb flux in lower slope sediments is expected to be 1.85 dpm/cm^2·y (Table 3.5). The values of J_{obs} in these cores (K-11 and M-12) are 1.29 and 0.64 dpm/cm^2·y respectively.

The observed flux of $^{210}Pb_{excess}$ is, therefore, both low and high relative to the expected value (Table 3.5). Similar results have been reported in an earlier study (Borole,1988). However, in the upper slope region at some selected sites, the $^{210}Pb_{excess}$ flux far exceeds the expected depositional flux. For example, at the core locations J-7 and 2502, the $^{210}Pb_{excess}$ flux is higher by a factor of three and four respectively. The ratio of observed to expected $^{210}Pb_{excess}$ fluxes in these cores is much lower than that reported in other margin regions such as Washington continental shelf and slope sediments (Carpenter et al,1981). Such higher supply of $^{210}Pb_{excess}$ flux to the Washington margin sediments has been explained through advection of seawater containing dissolved ^{210}Pb produced *in situ* from ^{226}Ra followed by enhanced scavenging (Carpenter et al,1981). A distinct difference in $^{210}Pb_{excess}$ flux in WCMI margin sediments and that in Washington shelf and slope regions is that at some sites along the WCMI, the observed values are significantly lower than the expected supply. This indicates that ^{210}Pb does not deposit at some sites due to high energy environment but gets focussed onto sediments at other sites. A significant positive correlation (r=0.89) has been observed between sediment accumulation rates and $^{210}Pb_{excess}$ inventory (I) in these sediments (Fig. 3.4).

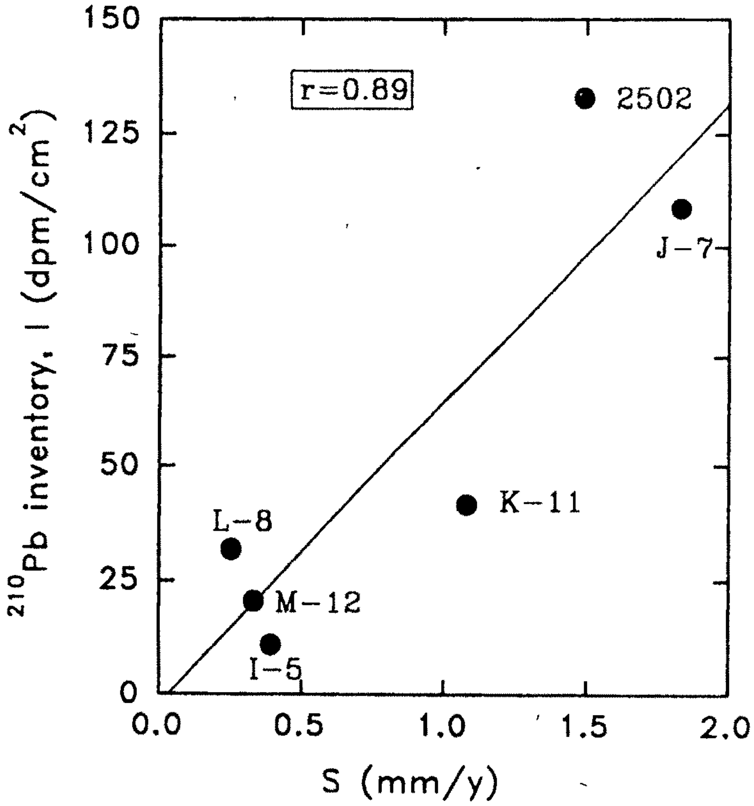

Figure 3.4: Scatter diagram of $^{210}Pb_{excess}$ derived sediment accumulation rates and $^{210}Pb_{excess}$ inventory in the sediment cores. The increasing $^{210}Pb_{excess}$ inventory with the sediment accumulation suggests focussing of ^{210}Pb along the margin sediments.

This enhanced $^{210}Pb_{excess}$ inventory is due to sediment focussing. These results point out that the source of ^{210}Pb to WCMI sediments is atmospheric but its deposition pattern is dependent on the accumulation rates of sediments.

3.4 Distribution of Mn in the WCMI sediments

It has been well documented that in anoxic marine sediments, where sediment accumulation is relatively high, manganese is mobilized as Mn(II) from the solid phase to solution (Lynn and Bonatti,1965; Holdren et al,1975; Jones and Murray,1985). In margin areas, the primary source of Mn to sediments is land-derived. Hence, one of the approaches to obtain information of Mn mobilization is to compare the abundances of Mn in margin sediments with that in the silicate matrix of the river-borne particles. The manganese concentration in sediments of the upper slope region of WCMI averaged over core length on a $CaCO_3$ basis (Table 3.6) varies from 285 to 350 ppm. This range of manganese concentration is similar to those reported earlier on surficial sediments of WCMI (Murty et al, 1978; Borole et al,1982a).

Table 3.6 : Mn concentration in the upper slope sediments on a $CaCO_3$ free basis.

Core: L-8

Depth (cm)	Mn (ppm)
(0-1)	349
(1-2)	316
(2-3)	303
(3-4)	308
(3-4)R	314
(4-5)	333
(5-6)	343
(6-7)	323
(8-10)	328
(10-14)	321
(18-20)	359
$\overline{Mn}$ =	327*

Core: J-7

Depth (cm)	Mn (ppm)
(0-2)	330
(2-3)	339
(3-4)	286
(4-5)	360
(5-6)	357
(6-7)	349
(9-10)	362
(10-12)	406
(14-16)	354
(18-20)	340
(20-22)	390
$\overline{Mn}$ =	352*

Core: I-5

Depth (cm)	Mn (ppm)
(0-2)	287
(2-4)	253
(4-6)	291
(4-6)R	273
(6-8)	310
$\overline{Mn}$ =	283*

* concentration averaged over entire core length
R denotes replicate analysis

The mean Mn concentration on a $CaCO_3$ free basis for the three cores studied is ~ 320 ppm, a factor of three lower compared to that reported in the river suspended particles (~1000 ppm) transported by the Narbada/Tapti rivers to this shelf region (Borole et al,1982a). The lower Mn concentration in these upper slope sediments could result from its preferential mobilization or due to dilution by biogenic and detrital components such as opal, organic matter, quartz etc. To determine if the low Mn concentration in the shelf sediments is due to dilution effects, the Mn/Al weight ratios in these cores have been compared with the Mn/Al ratios of the Narbada/Tapti river particles. As the Mn/Al ratios in these cores do not vary significantly with depth, the mean values taken over entire core lengths are compared with the Mn/Al weight ratio in the river-borne particles. The average Mn/Al ratios for these cores are: J-7 $(64\pm2)\times10^{-4}$, L-8 $(58\pm3)\times10^{-4}$, I-5 $(60\pm7)\times10^{-4}$ compared to values of 116×10^{-4} and 174×10^{-4} for the Narbada and Tapti particles (Borole et al,1982a). The Mn/Al weight ratio in river particles is higher by a factor of two to three compared to that of the upper slope sediments. Such a large difference in Mn/Al ratio can arise only due to the process other than dilution. The most likely mechanism for the low Mn content in the upper slope sediments is its reductive mobilization.

The mobilization of Mn from solid phase to solution in reducing sediments has been well documented (Lynn and Bonatti,1965; Trefrey and Presley,1982; Heggie et al,1987). Such mobilization influences the distribution of Mn in sediments and in seawater (Martin and Knauer,1984; Johnson et al,1992). Considering that the upper slope sediments are from reducing region and that dilution by biogenic and detrital components is not the cause of the low Mn abundance in them, it can be suggested that mobilization of Mn from solid phase to seawater under sub-oxic/anoxic conditions results in its low concentration. Also uniform distribution of Mn (Fig. 3.3) over the core length sampled for the upper slope sediments indicates that the sub-oxic/anoxic environment has remained unchanged over ~100–800 years BP.

For a typical sediment accumulation rate of 1 mm/y (typically observed in upper slope region, Table 3.5), a rough estimate of flux of Mn mobilized from these sediments can be obtained from the relation:

$$F_{Mn} = S \cdot \rho(C_r - C_s) \tag{3.12}$$

where F_{Mn} is the flux of Mn mobilized (μg/cm$^2\cdot$y), S is the sediment accumulation rate, ρ *in-situ* density, C_r and C_s are the Mn concentration in river particles ($\sim$ 1000 ppm) and in the upper slope sediments on $CaCO_3$ free basis ($\sim$ 350 ppm). The value of F_{Mn} is calculated to be 35 μg/cm^2·y. If the flux of Mn, as estimated above, is representative of an area 5^{0}lat×3^{0}long bounded by these cores, F_{Mn} is calculated to be ~5.0 × 10^{10} g/y which is nearly 15% of the dissolved Mn (~ 3 × 10^{11} g/y) transported by world rivers to ocean (Martin and Meybeck,1979). The estimated release of Mn from WCMI re-emphasizes the importance of the margin sediments in regulating the marine geochemical cycle of redox sensitive elements such as Mn. Furthermore, manganese mobilized from the upper slope region can be a potential source for the dissolved manganese maxima observed in the Arabian sea intermediate waters (Saager et al, 1989; Saager, 1994). However, it may also be possible that mobilization of Mn is occurring in the sub-oxic/denitrification layers from the sinking fluvial material or in the sediments. To understand and quantify the Mn mobilization from settling river particles through water column, it would be necessary to collect these particles using sediment traps and analyze them for Mn.

Table 3.7: The benthic manganese flux from margin sediments

Margin sites	Mn flux (μg/cm^2·y)	Reference
WCMI (upper slope)	~ 35	This study
Central California coast line	~ 10	Johnson et al, 1992
Gulf of St. Lawrence	~ 140–180	Sundby and Silverberg,1985
Mississippi Delta	~ 30–850	Trefry and Presley, 1982
Eastern Berring shelf	~ 1	Heggie et al, 1987

The flux of manganese solublized due to either of these proposed mechanisms vary from place to place (Heggie et al,1987; Johnson et al,1992). It is generally related to rates of sedimentation, biological productivity and also to the particle mixing by bioturbation (Aller, 1980). Johnson et al (1992) have reported that the average benthic flux (μg/cm^2·y) of Mn, (measured by using benthic chambers) from continental margin of Central California is supported predominantly by sinking particulate organic carbon and to a lesser extent by $CaCO_3$ dissolution. They have hypothesized that remineralization of organically bound Mn occurs primarily in a thin fluff layer (< 1 mm) at the sediment surface. Sundby and Silverberg (1985) have studied manganese cycling in Laurentian trough (water depth, 300–400 m) and applied a diagenetic modelling and mass–balance calculations to derive the Mn flux. They observed that only 13–29% of total manganese escaped from the sediment surface amounting to a net flux of 140–180 $\mu g/cm^2 \cdot y$ (Table 3.7). The magnitude of particle mixing by bioturbation was considered to be a deciding factor for increasing rate of Mn cycling both in the sediment core (internal cycling) and the fraction escaping to overlying waters.

Trefry and Presley (1982) have interpreted the deficiency of Mn in the Mississippi delta sediments, compared to that in the river particulates, as due to its mobilization under reducing conditions. Using the concentration gradient of Mn in sediment pore waters they calculated the outgoing diffusive manganese flux from sediments (water depth < 100 m) in the range of 30–850 $\mu g/cm^2 \cdot y$ (Table 3.7).

The low manganese concentration in the upper slope sediments by a factor of 3–4 compared to that transported through Narbada/Tapti river particles shows a clear indication of Mn mobilization from them to seawater. The pathways of Mn cycling and associated flux in upper slope sediments has been depicted in a schematic diagram, Fig. 3.5. The present study reemphasizes the importance of Mn cycling from anoxic shelf and slope sediments of the margin areas that can probably explain the source for the dissolved Mn maxima occurring in Arabian sea intermediate waters as mentioned earlier. This may also contribute to the high Mn concentration in the surface section of the lower slope sediments.

The manganese distribution in the two cores, K-11 and M-12, from the lower slope region shows features, which are distinctly different from those observed in the upper slope sediment cores, with high Mn values (1900 and 10160 ppm on $CaCO_3$ free basis) occurring in surface sections (Fig. 3.6, Table 3.8). In core M-12 the Mn concentration decreases with depth and attains a value of 900 ppm, for K-11 the Mn concentration shows a shallow depth (4–5 cm) maximum and then decreases to a value of $\sim$ 700 ppm below 10 cm depth. Such a distribution of Mn is typical of the slope sediments where Mn released at depths in sedimentary column by diagenetic processes is sequestered at the oxic sediment-water interface (Yeats et al,1979; Sundby and Silverberg,1985; Aller,1990). In contrast to the upper slope sediments, the concentration of Mn averaged over the entire core length for K-11 and M-12, is $\sim$1400 and $\sim$1700 ppm, respectively on a $CaCO_3$ free basis. These values of Mn are relatively higher than that in fluvial sediments transported by the Narbada/Tapti rivers and average crustal rock.

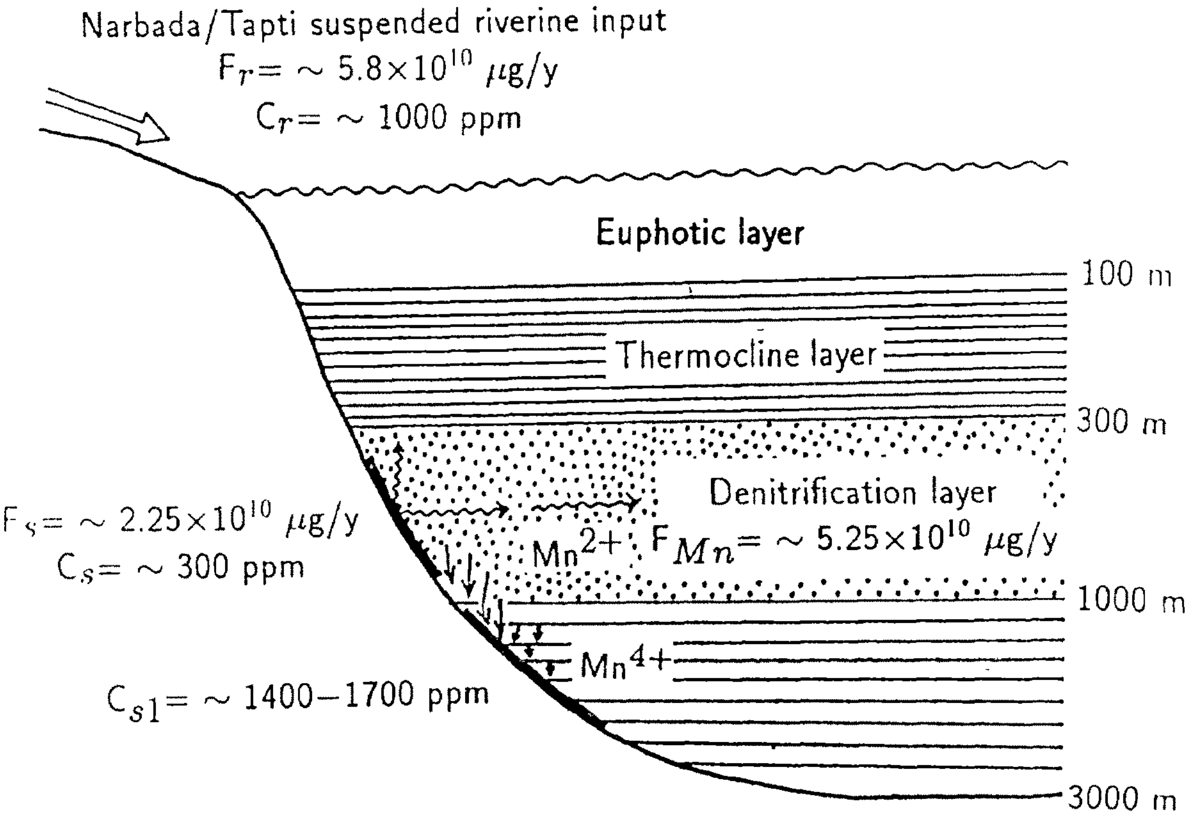

Figure 3.5: Schematic diagram showing Mn cycling between solid and aqueous phases in WCMI representing 5^0Lat×3^0Long area where : C_r is concentration and F_r the flux of Mn transported by riverine suspended matters. C_s and F_s refer to concentration and flux of Mn mobilized from reducing upper slope sediments to the denitrification layer. Further, C_{s1} is the average concentration of Mn observed in lower slope sediments. Although dissolved riverine Mn input and its atmospheric transport are neglected, a reasonable degree of balance is observed between F_r and (F_s + F_{Mn}). In the lower slope sediments, the mechanism for excess Mn depositing at the sediment-water interface due to upward migration from reducing sub-surface layers as well as its authigenic removal from overlying waters is also shown.

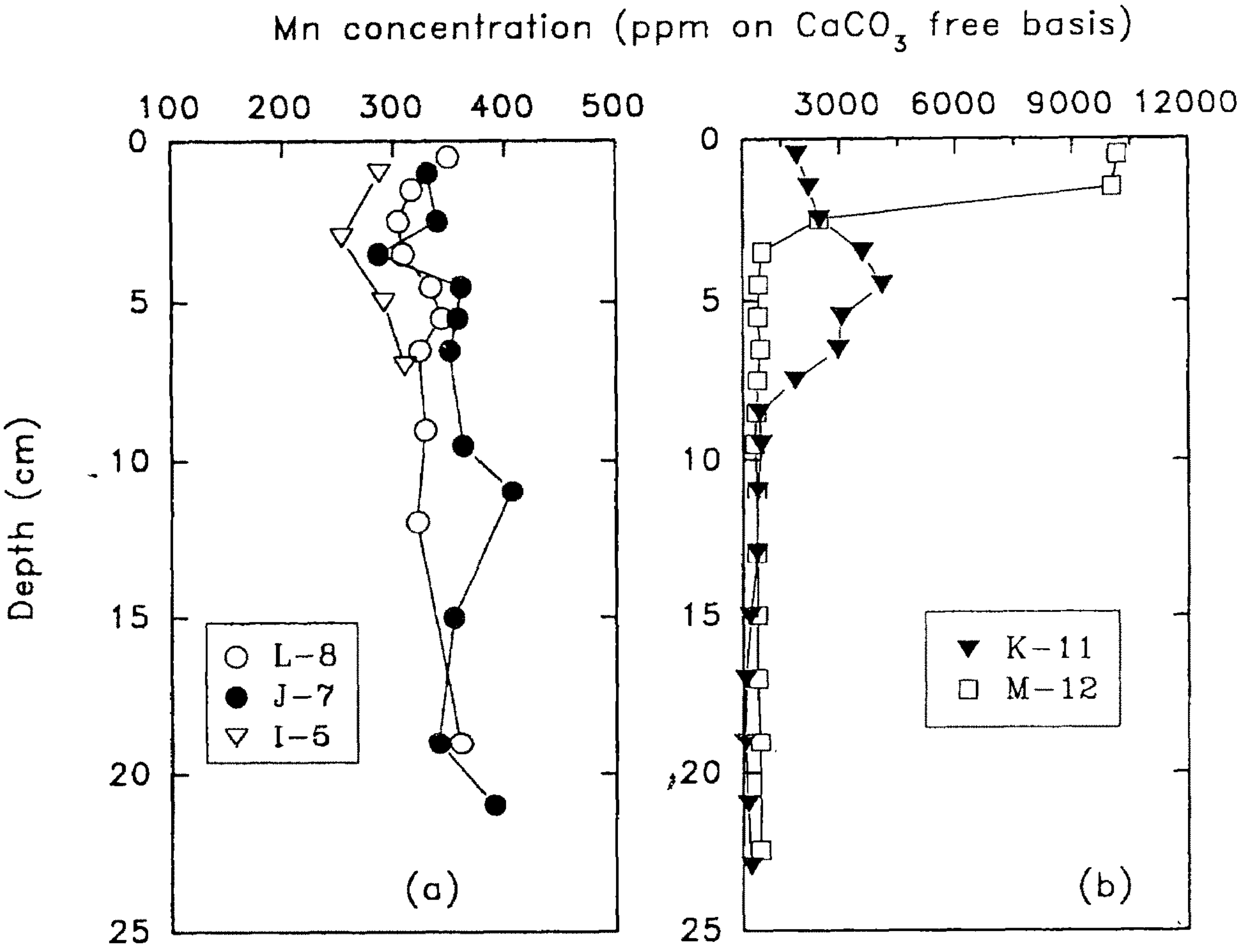

Figure 3.6: Downcore variation of Mn abundance in (a) the upper and (b) lower slope sediments. The Mn concentration in the upper slope sediments are much lower than that in the Narbada/Tapti river particles and show no discernible trend with depth. In contrast, the Mn distribution in the lower slope sediments show a distinct structure with high values near the sediment-water interface.

The bathymetric map of the study area (Fig. 2.1) indicates that the lower slope region follows closely the upper slope, and hence, it is reasonable to speculate that part of the manganese mobilized from the upper slope region is reprecipitated at the oxidising sediment-water interface in addition to that mobilized from the sub-surface layer. In fact, such a phenomenon has been reported to occur in other oceanic regions viz. the Gulf of

Mexico and Mississippi Delta (Trefry and Presley,1982; Heggie et al,1987).

3.4.1 Oxidation of Org. C and Mn reduction

The manganese reduction in nearshore sediments is represented by the following relation,(Aller,1990):

$$C_{org} + 2MnO_2 + 3CO_2 + 2H_2O = 4HCO_3 + 2Mn^{2+} \tag{3.13}$$

This shows that two moles of Mn^{+2} is generated during the oxidation of one mole of C_{org}. Therefore, it is possible to estimate the amount of C_{org} oxidized from the Mn^{2+} released based on this stoichiometry. The rough estimate of Mn flux mobilized from the upper slope, as discussed earlier, is ~0.6 $\mu M/cm^2 \cdot y$. This Mn, if attributed to C_{org} oxidation, would suggest that the oxidation rate for C_{org} in the upper slope region is ~ $0.3 \mu M/cm^2 \cdot y$. The primary production in upper slope region is about 0.5 $gC/m^2 \cdot d \equiv 1.5$ $mM/cm^2 \cdot y$ (Paropkari et al,1992). Comparing this with the C_{org} oxidation flux based on Mn reduction, it implies that reduction of Mn contributes to $< 1\%$ oxidation of C_{org} fixed by the photosynthetic activity.

In the lower slope sediments, the depth profile of "excess" Mn concentration can be represented by particle mixing and Mn reduction rate similar to that proposed by Aller,1980. This is represented by

$$\frac{\partial C_s^*}{\partial t} = D \cdot \frac{\partial^2 C_s^*}{\partial z^2} - R = 0 \tag{3.14}$$

Where D is the mixing coefficient, C_s^* is the solid-phase "excess" Mn concentration and R is the Mn reduction rate. It is assumed that D is constant over the depth interval used in the model calculation. The "excess" manganese (i.e. total solid-phase Mn minus the average background [1] value in $\mu g/g$) in top (0–4 cm) of the core M-12 is converted in units of mass/volume ($\mu M/cm^3$) by using in-situ sediment density of 0.5 g/cm^3 and its depth profile is fitted with an exponential function (Aller,1980):

---

[1] Background Mn concentration refers to unreactive Mn which remains almost constant after a certain depth from the surface

Table 3.8: Mn concentration in the lower slope sediments on $CaCO_3$ free basis.

Core: K-11

Depth (cm)	Mn (ppm)
(0-1)	1903
(1-2)	2211
(2-3)	2479
(3-4)	3581
(4-5)	4092
(5-6)	3052
(6-7)	2952
(7-8)	1862
(7-8)R	1841
(8-9)	922
(9-10)	975
(10-12)	881
(12-14)	865
(12-14)R	839
(14-16)	692
(16-18)	574
(18-20)	564
(20-22)	631
(22-24)	711
$\overline{Mn}$ =	1410*

Core: M-12

Depth (cm)	Mn (ppm)
(0-1)	10161
(1-2)	10017
(2-3)	2470
(3-4)	997
(4-5)	908
(4-5)R	930
(5-6)	897
(6-7)	947
(7-8)	889
(8-9)	847
(9-10)	810
(10-12)	865
(12-14)	864
(14-16)	884
(16-18)	887
(18-20)	944
(20-25)	958
$\overline{Mn}$ =	1705*

* concentration averaged over entire core length
R denotes replicate analysis

$$C_s^* = C_{so}^* \cdot e^{-\beta . z} \tag{3.15}$$

where C_s^* and C_{so}^* are the solid phase Mn concentration at any depth and at the sediment surface and β is the attenuation coefficient. The only unknown in eqn. (3.14) is D for determining (R), the Mn reduction rate. Assuming the exponential depth profile of $^{210}Pb_{excess}$ in top 10 cms of M-12 as solely due to particle mixing, the mixing coefficient D (Krishnaswami and Lal,1978), is calculated to be 0.18 cm^2/y. Using this value of D and exponential function for "excess" Mn concentration in eqn. (3.14) which results R, the Mn reduction rate. Integral of R over the depth interval for which "excess" Mn is observed, yields average Mn reduction flux of 0.45 $\mu M/cm^2 \cdot y$, and hence the flux of organic carbon oxidized from the sediment pile is $\sim$ 0.22 $\mu M/cm^2 \cdot y$.

As discussed above, a clear distinction exists for Mn distribution in sediments from the upper and lower slope regions mainly because of change in redox conditions. The depth profile of solid phase Mn in lower slope core M-12 was modelled with the particle mixing model (Aller,1980,1990), the result of which yielded carbon oxidation flux of 0.22 $\mu M/cm^2 \cdot y$. This estimated oxidative flux of organic carbon is nearly same compared to that of the upper slope anoxic sediments. The total carbon flux being oxidized from the WCMI sediments, ~ 0.52 $\mu M/cm^2 \cdot y$, is less than 1% of the primary productivity.

3.5 Distribution of uranium in slope sediments

In reducing marine environments, contrary to the mobilization of manganese, uranium is sequestered from seawater. As a result, the concentration of uranium is generally high in anoxic sediments (Veeh et al, 1967; Mo et al,1973; Cochran et al,1986 Anderson et al,1989; Barnes and Cochran,1990; Klinkhammer and Palmer,1991). The importance of such anoxic region as a potential sink for oceanic uranium has been a topic of discussion since long.

The abundance of uranium (^{238}U) in surface sediments of upper slope region ranges from 1.0 to 5.0 dpm/g on bulk basis (Table 3.2). The lowest concentration of uranium (~1 dpm/g) is observed in the I-5 core followed by that in 2502 (~3.0 dpm/g) and maximum concentration of ~ 5 dpm/g in L-8 and J-7 cores. The $^{234}U/^{238}U$ activity ratio in these sediments closely resembles that of seawater,1.14±0.02 (Koide and Goldberg,1965; Ku et al,1977; Chen et al,1986). Similar to this study, the concentration of uranium and its activity ratio ($^{234}U/^{238}U$) in surficial sediments from this region (ARB-46, ARB-52, ARB-54 and ARB-65H) have been reported earlier by Borole et al (1982b). They observed uranium concentration ranging from 3.9 to 7.5 ppm and its activity ratio identical to that of seawater value. The reported uranium concentration is higher than that in the Narbada/Tapti river particles by a factor of 3 to 6 and its maximum concentration is confined in the upper slope sediments. All these results strongly suggest that bulk of uranium in upper slope sediments is derived from seawater and hence this region acts as a potential sink for the dissolved uranium. The mechanism of high uranium content in the upper slope sediments is still not clear. The good correlation between ^{238}U concentration and LOI (organic matter) is suggestive of an association between these two constituents (Somayajulu et al,1994). However, from the present data it is difficult to discern if the association is genetic or due to the formation of sub-oxic/anoxic conditions in the sediments which help sequester uranium from seawater or it could be due to better preservation of C_{org} in high sedimentation region. It is also possible that part of the uranium in these sediments is derived from relict calcareous materials (e.g. oolites, corals, algal limestones and milliolites) present in the WCMI sediments (Rao,1978; Nair and Hashimi,1980). Some of these calcareous materials may have uranium concentrations ranging from 1 to 3 dpm/g (Sackett et al,1973; Baskaran,1985), similar to that has been found in this study in cores I-5 and 2502. The role of these upper slope sediments as a sink for authigenic uranium, however, is further discernible from the high ^{238}U/^{232}Th weight ratios (1 to 5, Fig. 3.7) in them compared to the average value for crustal rock, 0.25 (Gascoyne, 1982). Furthermore, Fig.3.7 shows almost uniform U/Th weight ratio (except L-8) throughout the core length, which attests to the earlier contention, based on solid phase Mn data, that reducing conditions in the upper slope region have remained fairly unchanged during the past ~100–800 years.

Based on uranium concentration in surface sediments and rate of sediment accumulation for upper slope sediments, the flux of uranium sequestered from seawater ranges between 30–550 μg/cm^2·ka. Since anoxic sediments are a potential sink for dissolved uranium supplied to ocean by world rivers, role of upper slope sediments from the WCMI could be significant in global perspective. The total dissolved uranium supply to ocean is 1.14×10^{10} g/y (Borole et al,1982b; Barnes and Cochran,1990; Sarin et al,1990). Considering typical U concentration of 5 ppm (usually found in upper slope sediments) depositing at a rate of 1 mm/y, the depositional flux of uranium is calculated to be 250 μg/cm^2·ka. Therefore, an upper limit for the amount of uranium depositing over an area of 5^0 lat× 3^0 long, 3.75×10^8 g/y, is about 3% of the total dissolved uranium supply to the ocean. Such an observation reemphasizes the importance of organic carbon rich margin sediments in balancing the input of dissolved uranium through world rivers. Klinkhammer and Palmer (1991) have estimated that nearly 75% of the dissolved uranium input to ocean is balanced by such margin sites and rest by the hydrothermal systems.

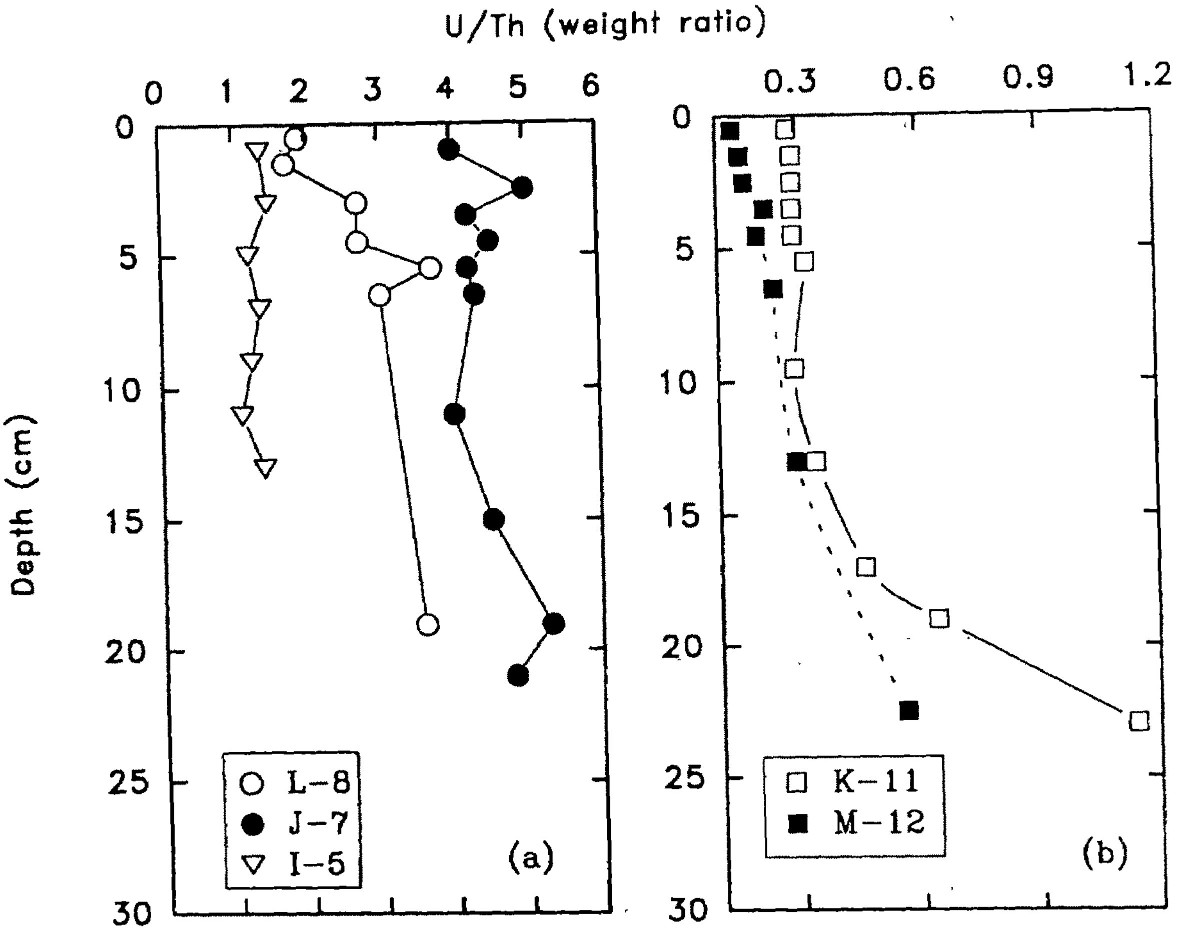

Figure 3.7: Downcore variation of U/Th weight ratio in (a) upper and (b) lower slope sediments. The upper slope sediments show that U/Th weight ratio remains almost constant with depth whereas the ratio increases with depth in the lower slope sediments.

In the lower slope region, the uranium concentration in surface sediments (K-11 and M-12) is about 1.0 dpm/g with activity ratio typically of 1.07±0.03 (Table 3.3). The low uranium abundance and its activity ratio in lower slope sediments (K-11 and M-12) present a distinction relative to the upper slope region which is most likely due to the oxidising conditions prevailing at the sediment-water interface. Such conditions are not favourable for authigenic deposition of uranium from seawater to the sediments. However, oxidation of organic matter may consume considerable amount of available oxygen resulting in sub-oxic condition deeper in the sediment pile. This may help in sequestering U from seawater to deeper depths of the sediment section. The reducing condition in deeper sediment section is evident from the solid phase Mn profile which shows low Mn concentration relative to the surface (Fig. 3.6). Therefore, increase in U/Th weight ratios (Fig. 3.7) with depth in these sediments is suggestive of U pumping from seawater to deeper depths. Such post depositional enrichment of U is also reported from other oceanic regions such as the Berring sea (Yamada and Tsunogai, 1983/1984). The exact mechanism of high U concentration at deeper depths can be understood if U is analyzed in sediment pore waters at various depths. It is to be noted that within the sediment pile, uranium shows a two component mixture as evidenced from activity ratio of uranium (1.07±0.03, Table 3.3) which is intermediate between detrital component and that of seawater.

3.6 Geochemistry of major and trace elements

Study on the distribution patterns of various major and trace elements in the sedimentary column provides useful information on the biogeochemical processes occurring in the sediments. Also, it is important to assess the role of recent anthropogenic inputs in modifying the natural input of various elements to margin areas via fluvial sediments. The various pathways of the pollutants (viz. anthropogenic heavy metals along with organic/inorganic materials) to the coastal regions are through direct dumping of sweage, river run-off and atmospheric contribution. The influence of anthropogenic activities is reflected through enrichment of heavy metals above a certain baseline value in surficial sediments of the coastal environment (Chow et al,1973; Bruland et al,1974; Goldberg et al, 1978,1979; Lyons et al,1983). It has been recognized that burning of fossil fuels has increased the concentration levels of Cu, Zn, Pb in certain coastal regions (Bruland et al,1974; Erlenkeuser et al,1974; Goldberg et al,1977; 1978).

A suite of elements viz: Fe, Al, Cu, Zn, Pb, and Ni were measured in the WCMI sediments (Tables 1A and 2A given in Appendix–A). Assuming Al as an index for silicates the abundances of various metals have been normalized with respect to Al in order to eliminate the diluent effects of $CaCO_3$ and OrgC. In the upper slope sediments, Cu/Al, Zn/Al and Fe/Al weight ratios range from $(11-22) \times 10^{-4}$, $(19-30) \times 10^{-4}$ and (0.64–0.76) respectively (Table 3.9). These metal to aluminum ratios are well within those reported for the Narbada/Tapti river suspended sediments (Borole et al,1982) thus indicating the dominance of fluvial source. The core I-5 shows exceptionally high Fe/Al (1.88), Ni/Al (56×10^{-4}) and Zn/Al (40×10^{-4}) ratios which could be attributed to relatively low abundance of clays. Borole et al,1982a have reported almost identical composition of Fe, Mn, Cu and Zn both in suspended bulk sediments and $< 4\mu$m fractions of the riverine suspended particles. These results suggest that the physico-chemical processes such as flocculation of particles, adsorption/desorption of metals on particulates do not modify significantly the elemental abundances of river borne particles during their transit through the estuarine regions of Narbada/Tapti rivers.

The association of various elements in margin sediments is understood by studying their inter-elemental correlations. For example, Mn, Ni, Cu, Zn and Pb in upper slope sediments show high positive correlations with Al (r: 0.72–0.99) suggesting that these elements get deposited along with the detrital clays. However, Ca shows strong negative correlation with Al (r=−0.97) indicating that its distribution is not controlled by the detrital clays and hence its source could be biogenic.

Table 3.9 Metal/Al ratios in WCMI sediments

metal/Al ratio	L-8	J-7	I-5	K-11	M-12
Fe/Al	0.64–0.76	0.69–0.75	1.60–1.88	0.67–0.78	0.66–0.72
Cu/Al	$(11-22)\times10^{-4}$	$(16-21)\times10^{-4}$	$(22-27)\times10^{-4}$	$(16-19)\times10^{-4}$	$(8-14)\times10^{-4}$
Zn/Al	$(19-30)\times10^{-4}$	$(20-23)\times10^{-4}$	$(32-40)\times10^{-4}$	$(19-22)\times10^{-4}$	$(14-19)\times10^{-4}$
Ni/Al	$(25-34)\times10^{-4}$	$(30-38)\times10^{-4}$	$(44-56)\times10^{-4}$	$(19-25)\times10^{-4}$	$(10-18)\times10^{-4}$
Pb/Al	$(18-22)\times10^{-4}$	$(19-28)\times10^{-4}$	$(30-42)\times10^{-4}$	–	–

The anthropogenic influence of heavy metals is generally inferred from their increasing concentrations towards the near surface sections by a factor of more than two with respect to bottom sections. Since the ^{210}Pb chronology established for the upper and lower slope sediment cores has yielded ages ranging between 100–800 years BP, therefore, these sediments can provide the pollution history during the last few centuries. For the upper slope region, Cu/Al, Zn/Al and Pb/Al ratios do not show any systematic increasing trend (Fig. 1A, given in Appendix–A). Such observations are contrary to the observed profiles of heavy metals in sediments from other coastal/estuarine regions viz. Chesapeake Bay, Baltic sea and Loch Etive (Scotland) (Erlenkeuser et al,1974; Goldberg et al,1978,1979; Ridgway and Price,1987), which have been reported to be affected by intense anthropogenic activities. In lower slope region, for the two cores (K-11 & M-12), the metal/Al ratios (Table 3.9) viz. Fe/Al: ~0.70; Cu/Al: (10–15) × 10^{-4}; Zn/Al: (18–20) × 10^{-4} and Ni/Al: (17–20) × 10^{-4} also agree very well with that of river borne particles (Borole et al,1982) and the upper slope sediments (this study). Also, similar to the upper slope region, there are no discernible increasing trend of metal/Al ratios with respect to bottom sections of the core (see Appendix–A, Fig. A2), thus indicating that anthropogenic inputs are relatively insignificant.

The depth profiles of Cu/Al and Pb/Al ratios in core L-8 show an increasing gradient and then decreases to baseline value at the surface (Appendix–A, Fig. A1). Such observation indicates that low Cu concentration at the core top is not due to the dilution effects caused by organic carbon and $CaCO_3$. The decreasing trend in either concentration of Cu or Cu/Al ratio near the sediment surface is probably related to the sub-oxic diagenetic mobilization of Cu, along with the manganese oxides, to overlying seawater (Klinkhammer,1980; Sawlan and Murray,1983).

It has been suggested that copper undergoes oxidative mobilization due to destruction or 'burning' of the organic copper carrier phase at the sediment-water interface (Klinkhammer,1980; Chester et al,1988). This mobilization of Cu gives rise to the high concentration of dissolved copper as reported by Heggie et al (1986) and Saager (1994) in seawater near the seafloor. The mobilization of copper from the lower slope region (core M-12) is quite evident from the low concentration of Cu or low value of Cu/Al ratio at the surface section of the core (see Appendix–A, Fig. 2A). The Zn/Al and Ni/Al ratios in K-11 have increased by about 25% at 5 cm depth with respect to the bottom sections. Such increase in Zn/Al and Ni/Al ratios coincide with increase in Mn concentration (Fig. 3.6) at that depth. It appears that Zn and Ni mobilized from deeper sections via pore waters are reprecipitated back in sediments along with Mn. The diagenetic geochemical behaviour of Ni and Mn is somewhat similar, as reported in an earlier study (Klinkhammer,1980). It can be inferred from the present study that Zn also probably undergoes diagenetic reactions similar to that of Mn and Ni.

Thus, the depth profiles of metal/Al ratios do not show a significant increase in the values at the core tops relative to the baseline in these margin sediments. These results show that the upper slope sediments of the eastern Arabian sea presently under the influence of reducing environment, have not been significantly perturbed by the recent anthropogenic activities during the last few centuries.

Chapter 4

Summary and Conclusions

Study of short sediment cores collected from the Western Continental Margin of India has provided important information on the temporal and spatial variability of biogenic components and geochemical behaviour of selected elements. The important conclusions of the present study are:

1. In general, sediments from the upper slope region are charaterized by the high abundances of $CaCO_3$ and Org. matter. $CaCO_3$, though biogenic in nature, its abundance in most of the cores is dominated by relict calcareous materials as evidenced by "older" ^{14}C ages (7200−4000 years BP) observed in various sections. Thus, $CaCO_3$ abundance in the upper slope sediments cannot be directly used as an index of biological productivity. Organic matter content in the upper slope sediments ranges from 7 to 15%, reflecting high biological productivity resulting from the upwelling of nutrient rich bottom waters and higher rates of sedimentation. The sediments from the upper slope region do not show any significant temporal variability with respect to $CaCO_3$; whereas in the lower slope its content varies as a function of depth by as much as 60%. It appears that the environmental conditions have not changed over the upper slope region during the last few centuries. For the lower slope region, it is difficult to identify the process involved in $CaCO_3$ variation, however, it is likely that $CaCO_3$ supply to sediments was relatively higher in the past.

2. The geochronology of the cores has been established based on the $^{210}Pb_{excess}$ method which yielded rates of sediment accumulation ranging from 0.25 to 1.83 mm/y for

the upper and lower slope sediments. The rate of sediment accumulation obtained for one of the cores from the upper slope sediments based on the ^{137}Cs depth profile is consistent with the value obtained from the ^{210}Pb method which ensures the ^{210}Pb chronology for all the cores. The inventory of $^{210}Pb_{excess}$ (Σ dpm/cm^2) along the margin ranges from 11 to 130 and shows a positive correlation with the sediment accumulation rate. These results suggest that ^{210}Pb deposition along the WCMI sediments is heterogenous and is focussed in regions of high sedimentation.

3. Geochemically, upper and lower slope sediments behave differently; the latter acts as a "sink" for oceanic uranium and a "source" for dissolved manganese to seawater. Sequestering of uranium from seawater to sediments and manganese mobilization out of sediments in upper slope sediments is largely controlled by the prevalent reducing conditions at the sediment-water interface. The uranium concentration of these sediments is typically 5 ppm with ^{234}U/^{238}U activity ratio of 1.14 ± 0.02, identical to that of seawater. In addition, the U/Th weight ratio in these sediments is quite high (1−5) compared to the average crustal value of 0.25. All these data suggest that uranium in these sediments is derived from seawater. Also, a near constancy in U/Th weight ratio down to about 25 cm depth implies that reducing condition at the sediment-water interface has remained unchanged since the last few centuries. An estimate of U being sequestered from seawater in the upper slope sediments of WCMI is nearly 3% of the dissolved U supply to the ocean via world rivers.

4. The flux of manganese mobilized from the upper slope sediments is of the same order as its dissolved supply to the ocean (3.0×10^{11} g/y) by the world rivers. The high flux of Mn mobilized from reducing sediments can possibly explain dissolved Mn maxima reported in the Arabian sea intermediate waters. The flux of labile organic carbon being oxidized from the margin sediments resulting from Mn reduction is $\sim$ 0.52 μM/cm^2·y which is less than 1% of the primary productivity.

5. The metal/Al ratios (Fe/Al, Cu/Al and Zn/Al) in margin sediments are similar to that reported for Narbada-Tapti river particles. Furthermore, a strong positive correlation exists between Cu, Zn, Ni, Pb and Al indicating that the distribution of

the trace elements is dominated by the fluvial sources. With no significant increase in either metal or metal/Al ratios of Cu, Zn, Pb and Ni at the core tops in these margin sediments relative to the bottom sections indicates that these metal concentrations are not significantly influenced by recent anthropogenic activities.

References

Aller R C and Cochran J K (1976) ^{234}Th/^{238}U disequilibrium in near-shore sediment : particle reworking and diagenetic time scale, *Earth Planet. Sci. Lett.*, **29**, 37–50.

Aller R C (1980) Estuarine Physics and Chemistry:Studies in Long Island Sound, pp 351–410. In: *Advances in Geophysics*, Diagenetic processes near the sediment-water interface of Long Island Sound II. Fe and Mn, Academic Press, Bary Saltzman (ed), **22**, Academic Press.

Aller R C, Benninger L K and Cochran J K (1980) Tracking particle-associated processes in near-shore environments by use of ^{234}Th/^{238}U disequilibrium, *Earth Planet. Sci. Lett.*, **47**, 161–175.

Aller R C (1990) Bioturbation and manganese cycling in hemipelagic sediments, *Phil. Trans. R. Soc. Lond.*, **A331**, 51-68.

Aller R C and DeMaster D J (1984) Estimates of particle flux and reworking at the deep-sea floor using ^{234}Th/^{238}U disequilibrium, *Earth Planet. Sci. Lett.*, **67**, 308–318.

Anderson R F, Bacon M P and Brewer P G (1983) Removal of ^{230}Th and ^{231}Pa at ocean margins, *Earth Planet. Sci. Lett.*, **66**, 73–90.

Anderson R F, Lehuray A P, Fleisher M Q and Murray J W (1989) Uranium deposition in Saanich Inlet sediments, Vancouver Island, *Geochim. Cosmochim. Acta* **53**, 2205-2213.

Bacon M P, Spencer D W and Brewer P G (1976) ^{210}Pb/^{226}Ra and ^{210}Po/^{210}Pb disequilibria in seawater and suspended particulate matter, *Earth Planet Sci. Lett.*, **32**, 277–296.

Barnes C E and Cochran J K (1990) Uranium removal in oceanic sediments and the oceanic U balance, *Earth Planet. Sci. Lett.*, **97**, 94–101.

Baskaran M (1985) Radiometric, mineralogical and trace elemental studies of the Saurastra quaternary carbonate deposits: Implications to their ages and origin, *PhD thesis*, Guj. Univ. (India)

Baskaran M, Sarin M M and Somayajulu B L K (1984) Composition of mineral fractions of the Narbada and Tapti estuarine particles and the adjacent Arabian sea sediments off western India, *Chem. Geol.*, **45**, 33–51.

Bassett J, Denney R C, Jeffery G H and Mendham J (1978) Vogel's textbook of quantitative inorganic analysis including elementary instrumental analysis, pp 320–321, The English Language Book Society, London.

Bhushan R, Chakrabarty S and Krishnaswami S (1994) Physical Research Laboratory (Chemistry) Radiocarbon Date list I, *Radiocarbon*, **36**, No. 2, 251–256.

Bonatti E, Fisher D E, Joensuu D O and Rydell H S (1971) Post-depositional mobility of some transition elements, phosphorous, uranium and thorium in deep-sea sediments, *Geochim. Cosmochim. Acta*, **35**, 189–201

Borole D V (1988) Clay sediment accumulation rates on the monsoon-dominated western continental shelf and slope region of India, *Mar. Geol.*,**82**, 285–291.

Borole D V, Sarin M M, Somayajulu B L K (1982a) Composition of Narbada and Tapti estuarine particles and adjacent Arabian sea sediments, *Indian J. mar. Sci.*, **11**, 51–62.

Borole D V, Krishnaswami S and Somayajulu B L K (1982b) Uranium isotopes in rivers, estuaries and adjacent coastal sediments of western India : their weathering, transport and oceanic budget, *Geochim. Cosmochim. Acta*, **46**, 125–137.

Brewer P G, Spencer D W, Biscaye P E, Hanley A, Sachs P L, Smith C L, Kadar S and Fredericks J (1976) The distribution of particulate matter in the Atlantic Ocean, *Earth and Planet. Sci. Lett.*, **32**, 393–402.

Bruland K W, Bertine K, Koide M and Goldberg E D (1974) History of metal pollution in the Southern California coastal zone, *Environ. Sci. Tech.*, **8**, 425–432.

Carpenter R, Bennett J T and Peterson M L (1981) ^{210}Pb activities in and fluxes to sediments of the Washington continental slope and shelf, *Geochim. Cosmochim. Acta*, **45**, 1155–1172.

Chen J H, Edward R L and Wasserburg G J (1986) ^{238}U, ^{234}U and ^{232}Th in seawater, *Earth Planet. Sci. Lett.*, **1986**, 241–251.

Chester R, Thomas A, Lin F J, Basham A S and Jacinto G (1988) The solid state speciation of copper in surface water particulates and oceanic sediments, *Mar. Chem.*, **24**, 261–292.

Chow T J, Bruland K W, Bertine K, Soutar A, Koide M and Goldberg E D (1973) Lead pollution : Records in Southern california coastal sediments, *Science*, **181**, 551–552.

Cochran J K, Bacon M P, Krishnaswami S and Turekian K K (1983) ^{210}Po and ^{210}Pb distributions in the central and eastern Indian Ocean, *Earth Planet. Sci. Lett.*, **65**, 433–452.

Cochran J K, Carey A E, Sholkovitz E R and Surprenant L D (1986) The geochemistry of uranium and thorium in coastal marine sediments and sediment pore waters, *Geochim. Cosmochim. Acta*, **50**, 663–680.

Delaune R D, Patrick Jr W H and Buresh R J (1978) Sedimentation rates determined by ^{137}Cs dating in a rapidly accreting salt marsh, *Nature*, **275**, 532–533.

Erlenkeuser H, Suess E and Willkam H (1974) Industrialization affects heavy metal and carbon isotope concentrations in recent Baltic sea sediments, *Geochim. Cosmochim. Acta*, **38**, 823–842.

Flanagan F J (1973) 1972 values for international geochemical reference samples, *Geochim. Cosmochim. Acta*, **37**, 1189–1200.

Gascoyne M (1982) Geochemistry of the actinides and their daughters, pp 33–55. In: *Uranium Series Disequilibrium Applications to Environmental Problems*, Ivanovich M and Harmon R S (eds.), Calrendon Press, Oxford.

Guinasso N L and Schink D R (1975) Quantitative estimates of biological mixing rates in abyssal sediments, *J. Geophy. Res.*, **80**, 3032–3043.

Goldberg E D and Koide M (1962) Geochronological studies of deep sea sediments by the ionium/thorium method, *Geochim. Cosmochim. Acta*, **26**, 417–450.

Goldberg E D and Griffin J J (1970) The sediments of the northern Indian Ocean, *Deep-Sea Res.*, **7**, 513–517.

Goldberg E D, Gamble E, Griffin J J and Koide M (1977) Pollution history of Narragansett Bay as recorded in its sediments, *Estuarine Coastal Mar. Sci.*, **5**, 549–561.

Goldberg E D, Hodge V, Koide M, Griffin J J, Gamble E, Bricker O P, Matisoff G, Holdren Jr G R and Barun R (1978) A pollution history of Chesapeake Bay, *Geochim. Cosmochim. Acta*, **42**, 1413–1425.

Goldberg E D, Griffin J J, Hodge V, Koide M and Windom H (1979) Pollution history of the Savannah River Estuary, *Environ. Sci. Tech.*, **13**, 588–594.

Gupta M V S and Hashimi N H (1985) Fluctuation in glacial and interglacial sediment discharge of the river Indus as seen in a core from the Arabian sea, *Indian J. Mar. Sci.*, **18(1)**, 66-70

Hermanson M H (1990) ^{210}Pb and ^{137}Cs chronology of sediments from small, shallow Arctic lakes, *Geochim. Cosmochim. Acta*, **54**, 1443–1451.

Heggie D, Kahn D and Fischer K (1986) Trace metals in metalliferous sediments, MANOP site M: interfacial pore water profiles, *Earth Planet. Sci. Lett.*, **80** , 106–116.

Heggie D, Klinkhammer G and Cullen D (1987) Manganese and copper fluxes from continental margin sediments, *Geochim. Cosmochim. Acta*, **51**, 1059–1070.

Holdren G R Jr., Bricker O P III and Matsoff G (1975) A model for the control of dissolved manganese in interstitial waters of Chesapeake Bay, pp 364–381. In:

Marine chemistry in the coastal environment, T. M. Church (ed.), A C S symposium series no. **18**.

Johnson K S, Berelson W M, Coale K H, Coley T L, Elrod V A, Fairley W R, Lams H D, Kilgore T E, Nowicki J L (1992) Manganese flux from continental margin sediments in a transect through the oxygen minimum, *Science*, **257**, 1242–1245.

Jones C J and Murray J W (1985) The geochemistry of manganese in the northeast Pacific ocean off Washington, *Limnol. Oceanogr.*, 30(1), 81–92

Klinkhammer G P (1980) Early diagenesis in sediments from the eastern equatorial Pacific, II. Pore water metal results, *Earth Planet. Sci. Lett.*, **49**, 81–101.

Klinkhammer G P and Palmer M R (1991) Uranium in the oceans: Where it goes and why, *Geochim. Cosmochim. Acta*, **55**, 1799-1806

Koide M and Goldberg E D (1965) $^{234}U/^{238}U$ ratios in seawater. In: *Progress in Oceanography* (ed M Sears), **3**, 173–179

Kolla V, Ray P K and Kostecki J A (1981) Surficial sediments of the Arabian sea, *Mar. Geol.*, **41**, 183–204.

Krishnaswami S (1976) Authigenic transition elements in Pacific pelagic clays, *Geochim. Cosmochim. Acta*, **40**, 425–434

Krishnaswami S and Sarin M M (1976) The simultaneous determination of Th, Pu, Ra isotopes, ^{210}Pb, ^{55}Fe, ^{32}Si and ^{14}C in marine suspended phases, *Anal. Chim. Acta*, **83**, 143-156.

Krishnaswami S and Lal D (1978) Radionuclide Limnochronology, pp 153–177. In :*Lakes: Chemistry Geology Physics*, Lerman A (ed.), Springer-Verlag, New York.

Ku T L, Knauss K G and Mathieu G G (1977) Uranium in open oceans : concentration and isotopic composition, *Deep-Sea Res.*, **24**, 1005–1017.

Lal D, Nijampurkar V N, Rajagopalan G and Somayajulu B L K (1979) Annual fallout of ^{32}Si, ^{210}Pb, ^{22}Na, ^{35}S and ^{7}Be in rains in India, *Proc. Indian Acad. Sci.*, **88**, 29-40

Lyle M and Dymond J R (1976) Metal accumulation rates in the southeast Pacific - errors introduced from assigned bulk densities, *Earth Planet. Sci. Lett.*, **30**, 164–168

Lynn D C and Bonatti E (1965) Mobility of manganese in diagenesis of deep sea sediments, *Mar. Geol.*, **3**, 457–474

Lyons W B, Armstrong P B and Gaudette H E (1983) Trace metal concentrations and fluxes in Bermuda sediments, *Mar. Pollut. Bull.*, **14**, 65–68.

Martin J M and Meybeck M (1979) Elemental mass-balance of material carried by major world rivers, *Mar. Chem.*, **7**, 173–206.

Martin J H and Knauer G A (1984) VERTEX: manganese transport through oxygen minima, *Earth Planet. Sci. Lett.*, **67**, 35–47.

Martin J M and Windom H L (1991) Present and future role of ocean margins in regulating marine geochemical cycles of trace elements, pp 45–67. In: *Ocean Margin Processes in Global Change*, Mantoura R F C, Martin J M and Wollast R (eds.), Wiley, Chichester.

Martin J M and Thomas A J (1994) The global insignificance of telluric input of dissolved trace metals (Cd, Cu, Ni and Zn) to ocean margins, *Mar. Chem.*, **46**, 165–178.

Mathieu, G G (1988) Systems for measurement of ^{222}Rn at low levels in natural waters. *Health Phys.*, **55**, 989–992.

Milliman J D and Meade R H(1983) World-wide delivery of river sediment to the oceans, *J. Geol.*, **91**, 1–21.

Milliman J D (1991) Flux and fate of fluvial sediment and water in coastal seas, pp 69–89. In: *Ocean Margin Processes in Global Change*, Mantoura R F C, Martin J M and Wollast R (eds.), Wiley, Chichester.

Mo T, Suttle A D and Sackett W M (1973) Uranium concentrations in marine sediments, *Geochim. Cosmochim. Acta*, **37**, 35–51.

Murty P S N, Rao M Ch, Paropkari A L and Topgi R S (1978) Distribution patterns of aluminum, titanium, manganese, copper and nickel in sediments of the northern half of the western continental shelf of India, *Indian J. Mar. Sci.*, **7**, 67–71

Naidu P D, Babu C P and Rao Ch M (1992) The upwelling record in the sediments of the western continental margin of India, *Deep-Sea Res.*, **39**, 715–723.

Nair R R (1969) Phosphotized oolites on the western continental shelf of India, *Proc. Nat. Inst. Sci. India*, **35**, 858–863.

Nair R R (1975) On the nature and origin of small-scale topographic prominences on the western continental shelf of India, *Indian J. Mar. Sci.*, **4**, 25–29.

Nair R R, Hashimi N H and Gupta M V S (1979) Holocene limestones of part of the western continental shelf of India, *J. Geol. Soc. India*, **20**, 411–420.

Nair R R and Hashimi N H (1980) Holocene climate inferences from sediments of the western Indian continental shelf, *Proc. Indian Acad. of Sci. (Earth Planet. Sci.)*, **89**, 299-315

Nair R R and Hashimi N H (1981) Mineralogy of the carbonate sediments– Western Continental Shelf of India, *Mar. Geo.*, **41**, 309–319.

Nair R R, Hashimi N H and Rao Purnachandar V (1982) Distribution and dispersal of clay minerals on the western continental shelf of India, *Mar. Geo.*, **50**, M1-M9.

Naqvi S W A (1994) Denitrification processes in the Arabian sea, *Proc. Indian Acad. Sci. (Earth Planet. Sci.)*, **103**, No. 2, 279–300.

Naqvi S W A, Noronha R J, Somasundar K and Sengupta R (1990) Seasonal changes in the denitrification regime of the Arabian sea, *Deep-Sea Res.*, **37**, 593–611.

Noshkin V E and Bowen V T (1973) Concentrations and distributions of long-lived fallout radionuclides in open ocean sediments, pp 671–686. In: *Radioactive Contamination of the Marine environment*, IAEA, Vienna.

Nozaki Y, Cochran J K and Turekian K K (1977) Radiocarbon and ^{210}Pb distribution in sub-mersible taken deep sea cores from Project Famous, *Earth Planet. Sci. Lett.*, **34**, 167-173.

Paropkari A L, Babuprakash C, Mascarenhas A (1992) A critical evaluation of depositional parameters controlling the variability of organic carbon in Arabian sea sediments, *Mar. Geol.*, **107**, 213-226.

Peirson D H (1971) Worldwide deposition of longlived fission products from nuclear explosions, *Nature*, **234**, 79–80.

Pennington W, Cambray R S and Fisher E M (1973) Observation on lake sediments using fallout ^{137}Cs as a tracer, *Nature*, **242**, 324–326.

Quasim S Z (1977) Biological productivity of the Indian Ocean, *Indian J. Mar. Sci.*, **6**, 122–137.

Ramswamy V, Nair R R, Manganini S J, Ittekkot V and Haake B (1991) Lithogenic fluxes to the deep Arabian sea measured by sediment traps, *Deep-Sea Res.*, **38**, 169-184

Rao Ch M (1978) Distribution of CaCO3, Ca^{2+} and Mg^{2+} in sediments of the northern half of western continental shelf of India, *Indian J. Mar. Sci.*, **7**, 151-154

Rao V P, Veerayya M, Nair R R, Dupeuble P A and Lamboy M (1994) Late Quaternary *Halimeda* bioherms and aragonitic faecal pellet-dominated sediments on the carbonate platform of the western continental shelf of India, *Mar. Geol.*, **121**, 293–315.

Ridgway I M and Price N B (1987) Geochemical associations and post-depositional mobility of heavy metals in coastal sediments : Loch Etive, Scotland, *Mar. Chem.*, **21**, 229–248.

Rosholt J N, Emiliani C, Geiss J, Koczy F F and Wangersky P J (1961) Absolute dating of deep sea cores by the ^{231}Pa/^{230}Th method, *J. Geol.*, **69**, 162–185.

Saager P M (1994) The biogeochemical distribution of trace elements in the Indian ocean, *Proc. Indian Acad. Sci. (Earth Planet Sci.)*, 103, 237-278.

Saager P M, DeBaar H J W and Burkhill P H (1989) Manganese and iron in Indian ocean waters, *Geochim. Cosmochim. Acta*, **53**, 2259-2267.

Sackett W M, Mo T, Spalding R F and Exner M E (1973) A reevaluation of the marine geochemistry of uranium, pp 757–769. In: *Radioactive contamination of the marine environment*, IAEA Symp. Proc.

Sarin M M, Borole D V and Krishnaswami S (1979) Geochemistry and geochronology of sediments from the Bay of Bengal and the equatorial Indian Ocean, *Proc. Indian Acad. Sci.*, **88**, Part II, 131–154.

Sarin M M, Krishnaswami S, Somayajulu B L K and Moore W S (1990) Chemistry of uranium, thorium, and radium isotopes in the Ganga–Brahmaputra river system : Weathering processes and fluxes to the Bay of Bengal, *Geochim. Cosmochim. Acta*, **54**, 1387–1396.

Sarin M M, R Bhushan, R Rengarajan and Yadav D N (1992) The simultaneous determination of ^{238}U series nuclides in seawater: Results from Arabian sea and Bay of Bengal, *Indian J. of Mar. Sci.*, **21**, 121–127.

Sarin M M, Krishnaswami S, Ramesh R and Somayajulu B L K (1994) ^{238}U decay series nuclides in the north eastern Arabian sea: Scavenging rates and cycling processes, *Continental Shelf Res.*, **14**, 251-265.

Sawlan J J and Murray J W (1983) Trace metal mobilization in the interstitial waters of red clay and hemipelagic marine sediments, *Earth Planet. Sci. Lett.*, **64**, 213–230.

Scott M R (1982) The chemistry of U and Th-series nuclides in rivers, pp 181–201. In: *Uranium Series Disequilibrium Applications to Environmental Problems*, Ivanovich M and Harmon R S (eds.), Calrendon Press, Oxford.

Shetye S R, Gouveia A D, Shenoi S S C, Sundar D, Michael G S, Almeida A M and Santanam K (1990) Hydrography and circulation off the the west coast of India during the Southwest Monsoon 1987, *J. Mar. Res.*, **48**, 359–378.

Shetye S R, Gouveia A D, Shenoi S S C, Sundar D, Michael G S, Almeida A M and Santanam K (1991) The coastal current off western India during northeast monsoon, *Deep-Sea Res.*, **38**, 1517–1529.

Sirocko F and Sarnthein M (1989) Wind–borne deposits in the northwestern Indian Ocean: Record of Holocene sediments versus modern satellite data, pp 401–433. In: *Paleoclimatology and Paleometeorology, Modern and Past patterns of Global atmospheric transport*, Leinen M and Sarnthein M (eds.).

Spencer D W, Bacon M P and Brewe P G (1981) Models of the distribution of ^{210}Pb in a section across the North Equatorial Atlantic Ocean, J. Mar. Res., **39**, 119–138.

Spitzy A and Ittekkot V (1991) Dissolved and particulate organic matter in rivers, pp 5–17. In: *Ocean Margin Processes in Global Change*, Mantoura R F C, Martin J M and Wollast R (eds.), Wiley, New York, N Y.

Somayajulu B L K, Yadav D N and Sarin M M (1994) Recent sedimentary records from the Arabian sea, *Proc. Indian Acad. Sci. (Earth Planet Sci.)*, **103**, No. 2, 315–327.

Sundby B and Silverberg N (1985) Manganese fluxes in the benthic boundary layer, *Limnol. Oceanogr.*, **30(2)**, 372–381.

Thomson J, Colley S, Anderson R, Cook G T and MacKenzie A B (1993) ^{210}Pb in the sediments and water column of the northeast Atlantic from 47 to 59^{0}N along 20^{0}W, *Earth Planet. Sci. Lett.*, **115**, 75-87.

Trefry J H and Presley B J (1982) Manganese fluxes from Mississippi Delta sediments, *Geochim. Cosmochim. Acta*, **46**, 1715–1726.

Veeh H H (1967) Deposition of uranium from the ocean, *Earth Planet. Sci. Lett.*, **3**, 145–150.

Walsh J J (1991) Importance of continental margins in marine biogeochemical cycling of carbon and nitrogen, *Nature*, **350**, 53–55.

Wollast R (1991) The coastal organic carbon cycle: Fluxes, sources and sinks, pp 365–381. In: *Ocean Margin Processes in Global Change*, R F C Mantoura, J M Martin and R Wollast (eds.), Wiley, Chichester.

Wollast R (1993) Interaction of carbon and nitrogen cycles in the coastal zone, pp 195–210. In: Interaction of C, N, P and S biogeochemical Cycles and Global Change, R Wollast, F T Mackenzie and L Chou (eds.), NATO ASI Ser., **14**, Springer, Berlin.

Yadav D N, Sarin M M and Somayajulu B L K (1992) Western Continental Margins of India: Are they sink or source for trace elements in the Arabian sea ?, pp 359–367. In: *Oceanography of the Indian Ocean*, Desai B N (ed.), Oxford & IBH Pub. Co., New Delhi.

Yamada M and Tsunogai S (1983/1984) Post depositional enrichment of uranium in sediment from the Berring sea, *Mar. Geol.*, **54**, 263–276.

Yeats P A, Sundby B and Bewers J M (1979) Manganese recycling in coastal waters, *Mar. Chem.*, **8**, 43–55.